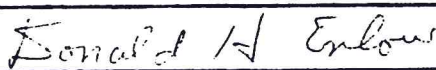CASE WESTERN RESERVE UNIVERSITY

GRADUATE STUDIES

We hereby approve the thesis of

ISARAVADEE UDOMSIRI-VISETSIRI

candidate for the Master of Science in Dentistry
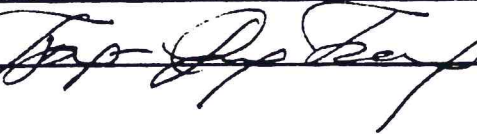
degree.

Signed: _____
(Chairman)

_____
Donald H Enlow

_____
Elaine K Keeler

_____

Date   May 9, 1988.

MAGNETIC RESONANCE IMAGING AND

FUNCTIONAL ANALYSES OF MASTICATORY BIOMECHANICS

by

ISARAVADEE UDOMSIRI-VISETSIRI

Submitted in partial fulfillment of the requirements

for the Degree of Master of Science in Dentistry

Department of Orthodontics

School of Dentistry

CASE WESTERN RESERVE UNIVERSITY

May 1988

MAGNETIC RESONANCE IMAGING AND
FUNCTIONAL ANALYSES OF MASTICATORY BIOMECHANICS

Abstract

by

ISARAVADEE UDOMSIRI-VISETSIRI

Physiological cross-sectional areas of the jaw elevator muscles were determined in fifteen vervet monkeys by means of magnetic resonance imaging and "instant oblique reconstruction," a data manipulation procedure for obtaining cross-sectional characterizations in a specific plane. To increase variability in masticatory parameters, ten animals were maintained on a hard diet, while five were fed a soft diet. The data gathered by magnetic resonance imagery were compared with data collected by a variety of other methods, including bite force measurement and standard radiographic cephalometry and measures including such masticatory parameters as lever arm length, load arm length and a mechanical efficiency index. Data obtained through these combined techniques were analyzed by correlation analysis, the Student's t-test, and analysis of variance.

The resulting correlations between the cross-sectional areas of the jaw elevator muscles are at the same level as correlations that have been recorded in human studies, confirming the assumption that the vervet monkey is a good animal model of human craniofacial biomechanics. Significant correlations ($p < .05$) found between

parameters of the masticatory system included the following: maximum elicited _in vivo_ bite force and cross-sectional areas of the masseter muscle at the level of $r^2 = 0.35$, of the medial pterygoid at the level of $r^2 = 0.24$, and of the temporalis at the level of $r^2 = 0.17$; masticatory lever arm lengths with masticatory load arm lengths at the level of $r^2 = 0.91$. Masticatory-lever arm lengths correlated with the cross-sectional areas of the masseter muscle at $r^2 = 0.59$, with the temporalis muscle at 0.32. Correlations of 0.44 and 0.69 were observed between maximum bite force and chronological age, and bite force and body weight in monkeys raised on a "hard" diet. In monkeys raised on a "soft" diet, these correlations were reduced to 0.35 and 0.58 respectively.

The magnetic resonance imaging methodology proved suitable for this unique, quantitative analysis. Results obtained in this study provide baseline information for further studies of masticatory biomechanics by establishing quantitative measurements of biomechanical variables. This type of study and the kinds of information that it can yield shows potential for significant applications in craniofacial biology and has obvious implications for use in areas of orthodontics and craniofacial surgery.

DEDICATED

TO

My parents and my brother, Apiwat, who sacrified many things

so that I could pursue an education.

and

My husband, Sompop, whose love, support, and encouragement

made this accomplishment possible.

ACKNOWLEDGEMENTS

TABLE OF CONTENTS

PAGE

LIST OF TABLES

LIST OF FIGURES

x

INTRODUCTION AND LITERATURE REVIEW

The present investigation is one of the first attempts ever to use Magnetic Resonance Imaging to enhance our understanding of masticatory biomechanics. This study is part of a longitudinal experimental study of the effects of masticatory biomechanics on the growing craniofacial skeleton. The broader study is directed at clarifying the relationship between masticatory muscle function and craniofacial growth. It has been in progress for several years. The present independent study focuses on a methodology which proposes to establish and clarify the relationship between muscle function and craniofacial growth by means of magnetic resonance imaging. Quantitative measures arrived at through magnetic resonance techniques have been correlated with measurements of masticatory bite force and of structural configurations in the craniofacial skeleton of a population of experimental animals. The data from such correlations yield a baseline for biomechanical models which can answer some specific questions about masticatory biomechanics. The questions being considered include, "What can these methods tell us about the biomechanics of mastication?" "What are the relationships among the cross-sectional areas of those muscles (the temporalis, the medial pterygoid, and the masseter) which elevate the jaw?" "What are the relationships among the cross-sectional areas of masticatory muscle, masticatory aspects of facial size and shape, and the bite force capabilities of growing monkeys?" "How do these parameters

1

change during growth?" "How do the craniofacial skeleton and the masticatory muscles change in order to accommodate the bite force capabilities?" In this report, it will be shown that magnetic resonance imaging techniques and the data they produce presently make it possible to undertake new analyses that expand our understanding of how the growing facial skeleton is able to respond to changing circumstances. This study should contribute to a clearer understanding of craniofacial mechanics and of facial development and should, therefore, provide answers to pressing clinical problems in orthodontics and craniofacial orthopaedics.

Following is a brief review of the fundamental concepts of facial growth and masticatory biomechanics upon which this study is based.

Over the past century, many investigators in the fields of orthodontics and craniofacial biology have attempted to achieve a basic understanding of craniofacial growth and development. The work of Enlow, Frankel, McNamara, Moss, Scott, Sicher, Woodside, and others (see below), has contributed significantly to our knowledge in this area, without, however, arriving at any definitive explanation of the correlation between the structural and functional aspects of craniofacial growth. Any explanation of why the face grows in a particular way must entail a description of exactly what happens during facial growth. As Oyen (1988) points out, such an explanation must identify and relate the structural and functional needs that are being served and recognize and account for any alterations in those

needs as they occur. There are theories which have attempted to do this.

Numerous investigations of the living and skeletal primate populations' craniofacial area have been conducted in order to explain relationships between craniofacial growth and masticatory function. The muscles of the craniofacial complex have always been of central concern to craniofacial biologists and clinicians, primarily because of the influence of muscle function on the growth and form of the craniofacial skeleton (Carlson, 1983). Some studies have employed surgical methods to clarify the role of muscle function and craniofacial morphology. Varous investigators conducted ablative studies of the temporalis muscle (Washburn, 1947; Horowitz and Shapiro, 1951; Moss and Meehan, 1970; Soni and Malloy, 1974), or the masseter muscle (Pratt, 1943; Horowitz and Shapiro, 1955; Avis, 1961). These studies demonstrate skeletal changes in response to surgical removal of muscle attachment, contradicting the findings of Anthony (1903), who removed the temporal muscle from one side in very young dogs and, by comparing the altered side to the normal side, found that the bone on the operated side thickened in the absence of the temporal muscle. Nikitius confirmed Anthony's results and demonstrated that the cranium became thicker on the operated side in dogs (1965) and rhesus monkeys (1964). Alternative interpretations have been offered in which it was suggested that interruption of the neuro-vascular supply to the bone causes skeletal changes (Horowitz and Shapiro, 1951; Boyd et al., 1967; Johnson, 1976).

Further investigation of bone-muscle relationships occurs in research involving treatment with functional appliances. Functional appliances were first developed by Andreson and Haupl (1936), who assumed that anticipated skeletal adaptation would result from intrinsic remodeling responses subsequent to environmental changes that we are not wholly dependent on to extrinsic mechanotherapy. Studies in which the position of the lower jaw was altered by use of functional appliances in growing monkeys showed that the muscle plays an active role in determining the antero-posterior position of the mandible (McNamara, 1972, 1973, 1984; McNamara and Carlson, 1979). Through functional protrusion experiments, they have shown that facial skeletal growth can be changed significantly through altering the biomechanical and biophysical environment of the craniofacial complex. These results led Fränkel (1980) to reiterate that local biomechanical conditions can be altered by craniofacial orthopaedics.

In spite of these experimental and clinical endeavors, the problem of the extent craniofacial morphology is affected by masticatory biomechanics has not, thus far, been adequately explained and is still a matter of considerable controversy. Studies have been directed at relating craniofacial morphology with electromyographic activity in the facial and masticatory musculature and measurement of bite force (e.g. Ralston, 1961; Ahlgren and Owall, 1970). Many studies have been carried out to calculate bite force. Review articles in this field are given by Brawley and Sedwich (1940), Strenger (1949), Jenkins (1966) and others. The measurement of

forces in the oral cavity has evolved from the use of relatively crude mechanical measuring devices placed between the teeth to the improved strain gage technology with leads to the recording equipment. Using such technology, Linderholm and Wennstrom (1970) found no correlation between bite force and general muscle force or body build in young males; in children, only weak correlation was seen. Ringquist (1973) showed correlations in young women among bite force and facial morphology and electromyographical activity. In 1978, Ingervall et al. studied the facial morphology of fifty men with strong and weak bite force. Their findings support the hypothesis that the facial morphology partly depends upon the strength of the masticatory muscles. In contrast, Throckmorton et al. (1980) found that the bite force level may be the result of the geometric arrangement of the lever system of the jaws. When the gonial angle is obtuse and the mandibular plane is steep, the elevator muscles of the mandible are at a mechanical disadvantage. Throckmorton and his colleagues support this finding that the functional parameters of the masticatory muscles vary with the form of craniofacial skeleton.

The relation between the craniofacial skeleton and muscle architecture has also been assessed. In 1984, Weijs and Hillen described the relationship between "Physiological Cross-Section" obtained through autopsy of the human masticatory muscles and cross-sectional area reconstructed from computer tomograms. In their study, it was shown that the cross-sectional areas of masticatory

muscles measured in tomograms taken at predefined levels in each muscle are proportional to the total fiber cross-sectional area determied from cadavers. In 1986, Weijs and Hillen used twenty-nine adult human subjects to determine the correlation between cross-sections of jaw muscles (measured in computer tomography scans) and a number of characteristic facial dimensions. Their results support the hypothesis that jaw muscles affect facial growth and, in part, determine the final facial dimensions. In 1984, Takada et al. analyzed the orientation of the superficial masseter and temporalis muscles relative to dentofacial morphology using head films. The muscular origins and insertions were identified through examination of dry skulls using anatomic and geometric criteria. In this study, it was suggested that a positive association exists between the inclination of masseter muscle and the steepness of the occlusal plane.

The relationship between muscle function and the size and shape of the craniofacial skeleton has been studied in rats by feeding them hard and soft diet (Watt and Williams, 1951; Barber, Green and Cox, 1963). Investigators found that size of the mandible and transverse width of the maxilla were affected in the soft diet animals. Kiliaridis (1985) reported that changes were induced in the craniofacial growth of rats fed a soft diet and suggested that these changes were related to the low forces developed by the under-exercised masticatory muscles of the soft diet group. Cavalancia (1985), in a preliminary analysis of the palatal

dimensions of monkeys kept on a dietary regime, found that, after eighteen months on a soft diet, palatal length increased relatively and palatal breadth became relatively narrower than those of monkeys fed a hard diet. While a number of measurements have been taken from animals in dietary consistency experiments, there has been no attempt to integrate these data in such a way that interactions between different parts of the growing masticatory systems could be measured (Beecher and Corruccini, 1981).

Attempts to evaluate craniofacial biomechanics have employed populational and longitudinal craniometric data (Endo, 1966; Hylander, 1972, 1977; Oyen et al., 1979, 1982; Russell, 1983; Rangel et al., 1985). Oyen (1982) studied the masticatory function and histogenesis of chimpanzees skulls. Results obtained by these investigators support the notion that morphogenesis of the upper face is significantly affected by growth-related alterations in masticatory function. In studies using vervet monkeys, measurements of some components of biomechanical analyses were taken directly from dry skulls, with lever arms and load arm lengths calculated from muscle attachment markings or morphological landmarks (Oyen et al., 1979, 1982; Russell, 1983; Rangel et al., 1985). Since masticatory muscle force cannot be measured directly in dry skulls, it was assumed in these studies that total masticatory muscle force is highly correlated with temporalis muscle cross-section, which was estimated by reconstructing and measuring the area of the temporal or zygomatic fossa. A mechanical efficiency index (percentage ratio of

the lever arm to the load arm) was calculated to estimate the bite force potential which acted upon the craniofacial skeleton at various positions in the dental arch (Oyen, 1982; Russell, 1983; Rangel et al., 1985.). Rangel and her colleagues also found that changes in biomechanics of the masticatory apparatus affect local remodeling responses seen in the supraorbital region, with skeletal growth responses reflecting changes in masticatory force. Individuals with a reduced efficiency index were likely to have a greater than average total area in the supraorbital region.

The functional matrix theory (Moss and Young, 1960; Moss, 1962) offers a sound approach to the questions of how and why the face grows as it does; but this theory lacks the quantitative approach that is necessary to a precise understanding of the functional aspects of facial growth and development. Studies (described above) which have employed such diverse methods as surgical alteration, altered function, and electromyographic activity were not intended to sufficiently delineate the biomechanics of the masticatory system. This seems traceable to an inability to proceed towards a more effective way to understand the basic biological mechanism.

In order to achieve the construction of biomechanical models in primates, longitudinal studies are needed. Measurement of maximum and normal bite forces and assessment of muscle forces and masses should determine the validity of the biomechanical models. Further

studies that use advanced technology, such as this one, are obviously needed.

The idea of using nuclear magnetic resonance was suggested in 1946 by Edward M. Purcell of Harvard University and Felix Bloch of Stanford whose discovery of the resonance properties of atomic nuclei within a magnetic field earned them the Nobel Prize for Physics in 1952. The method enlists the phenomenon of nuclear magnetic resonance which allows radiowaves to be transmitted and detected in the presence of a magnetic field. Since different tissues have different radiofrequency characteristics, it is possible to transform the variations in radiofrequency signals into tissue images. In 1971, Damadian was the first to study biopsied samples of cancerous tissues, finding that the image intensity varied from normal tissues (Damadian, 1971). Lauterbur (1972) demonstrated the first two-dimensional image of the proton density in a water sample and showed how an magnetic resonance signal could be changed into an visual image by using a reconstruction method. Mansfield et al., 1976, demonstrated human anatomical detail _in vivo_ by a line-scanning technique. At present, this noninvasive diagnostic technique is commonly known as Magnetic Resonance Imaging. It has been widely applied in many areas of medical research due to its ability to visualize both hard and soft tissue structures.

In 1985, Case Western Reserve University's School of Dentistry and the Picker International Clinical Research Center established a cooperative affiliation in order to undertake a related

series of investigations of masticatory functional anatomy. With additional support from the National Science Foundation, Drs. O. J. Oyen and M D. Russell established a pilot study of two humans and two live monkeys by using magnetic resonance imaging to characterize the muscle vectors acting on the craniofacial facial skeleton. This report is a direct outgrowth of the pilot study. Prior to this investigation, no quantitative analysis of the living masticatory system using magnetic resonance imaging has been published.

We still do not completely understand the structural-functionalism significance of masticatory biomechanics. We also do not really understand the causal mechanisms of relapses in orthodontics. Functional appliances, an important innovation in orthodontics, are still very controversial, with major arguments centering on whether skeletal adaptation results from intrinsic remodeling responses or from extrinsic mechanotherapy. To answer specific questions concerning how to apply a specific appliance, we need to obtain precise information that has, thus far, not been available to the orthodontist.

The primary goal of this investigation is not to fabricate a specific method of treatment in orthodontics. Rather, if this study realizes its goal, it will contribute to a clearer understanding of craniofacial biomechanics and of facial development and will facilitate the attainment of answers to pressing clinical problems related to orthodontics and craniofacial orthopedics.

MATERIALS AND METHODS

Fifteen growing male African green or vervet monkeys (Cercopithecus aethiops) were used in this study (Figure 1). These animals were wild-caught on the island of St. Kitts and have been part of a long term evaluation of the relationship between mastication and facial growth that began in 1983. Because only males were used, it was possible to control for genetic factors and hormonal levels. The green monkey was chosen for study because its masticatory system is generally comparable to that of other primates, including humans. Due to this similarity, there is considerable biologic information already available about another Cercopithecine monkey, the rhesus macaque.

At the time of capture, the monkeys were infants or young adolescents. At the time of initial magnetic resonance imaging data acquisition in 1987, the monkeys were approaching dental maturity, i.e. nine animals had functioning third permanent molars, all animals had functioning second permanent molars and functional permanent canines. Three monkeys had impacted third permanent molars. When the magnetic resonance imaging data acquisitions were repeated in 1988, one animal had functioning second permanent molars, eleven animals had functioning third permanent molars and three animals had impacted third permanent molars.

Since the animals were wild-caught, their chronological ages were unknown but they have been estimated on the basis of stages of dental eruption according to procedures used in earlier studies

11
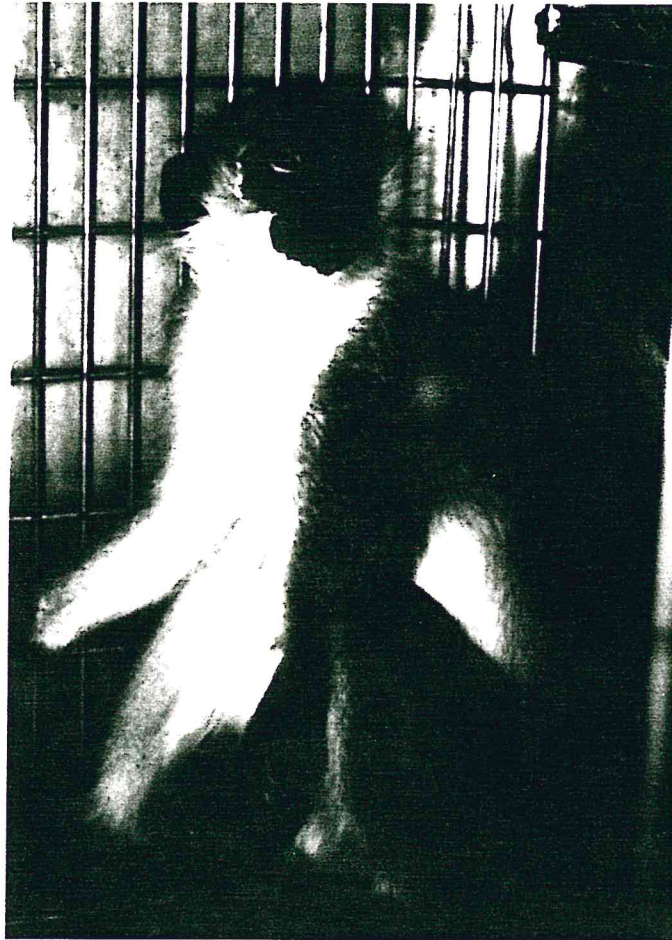
Figure 1. African green or vervet monkey
(Cercopithecus aethiops).

TABLE I. The Estimated Chronological Age of the Monkeys According
to Dental Status at the Onset of the Experiment

Estimated Chronological Age

Group	Number	Dental Age	Estimated Age (mos.)
I	5	Full deciduous teeth	11
II	8	M1 in occlusion	13
III	2	M2 in occlusion	28

(Oyen, 1984; Oyen et al, 1979; Oyen and Rice, 1980). The estimated ages at the onset of the experiment are represented in Table 1.

Since the onset of the study, the monkeys have been individually housed in cages specially designed for long-term maintenance of small primates. Feeding and care of the monkeys has been monitored at least twice daily over the length of the entire study. These services have been provided by the Animal Resource Center of Case Western Reserve University.

To increase variation in bite force capabilities, as per the original research protocol, the monkeys were subdivided into two groups and maintained on contrasting "hard" and "soft" diets of identical nutritional value. At the time of the first magnetic resonance imaging data gathering session the monkeys had been on these diets for approximately 36 to 40 months. Further details are as follows.

Experimental Group I: hard diet. Ten monkeys have been maintained on a hard diet adapted from the procedures used with considerable effectiveness in previous experimental studies of rats by Watt and Williams (1951), Barber et al. (1963), and of primates by Beecher and Corruccini (1981), Ward et al.(1981) and Bouvier and Hylander (1981). The hard diet consists of nutritionally balanced, commercially prepared hard biscuits, augmented periodically by unpeeled apples. Although the biscuits are sufficiently enriched to meet the nutritional requirements of growing monkeys, apples have been regularly provided because of their relative hardness and their

resistance to softening through retention in the oral cavity or buccal pouch before actual chewing. Moreover, Hylander (1979) has shown that mastication of apple skins involves the generation of significant levels of bite force and bone strain. Water has been available on an ad libitum basis.

Experimental Group II: Soft Diet. Five animals have been maintained on a soft diet whose consistency has been softened to induce alterations in levels and patterns of masticatory bite force. This diet has the consistency of soft fudge and requires no mastication. It consists of liquified Purina monkey chow, vitamin supplement, applesauce and fruit cocktail or preserved fruit segments, e.g. canned peach segments.

The teeth and gingiva of each monkey in both diet groups were routinely examined every six to eight weeks for the presence of dental calculi or tissue inflammation that might modify masticatory function.

Data Collection

Part I: Cephalometric evaluation.

While a broad variety of cephalometric procedures, including surgically placed metallic implants, were used as part of the long-term study, for purposes of this analysis, cephalometric procedures were limited to characterizing specific atributes of the masticatory system. Lateral cephalograms were obtained from each

monkey according to established radiographic procedures in the following manner:

The monkey was first administered general anesthesia with a combination of Xylazine (Rompun) 1.5 mg, Atropine sulfate .05 mg and Ketamine hydrochloride 1.5 mg per kilogram body weight. The animal was then positioned and secured in an especially designed cephalostat (Figure 2). The ear rods were placed in the external auditory meatus, and the head was then positioned along the Frankfort horizontal plane. Kodak type M film was used to enhance visualization of detail.

Cephalograms were obtained at approximately the same time as data about magnetic resonance imaging and bite force. All roentgenograms were traced with a Pentel technical pen (0.3mm lead) on 0.076mm matte acetate paper. Figure 3 identifies anatomical structures seen on a typical lateral cephalometric roentgenogram. For purposes of registration during comparison of radiographs obtained at different ages, the radiographs were oriented on the basis of the cranial base and its implants.

Measurements were taken with a Helios dial caliper, graduated to 0.05mm. Readings were recorded to the nearest 0.1mm Also, all measurements were recorded with the Hi-Pad digitizer and Bioquant Software and an Apple IIe computer.

Selected parameters of the masticatory system were measured from periodic cephalographs according to the procedures used in previous studies (Oyen et al, 1979, 1982; Russell, 1983; Rangel,
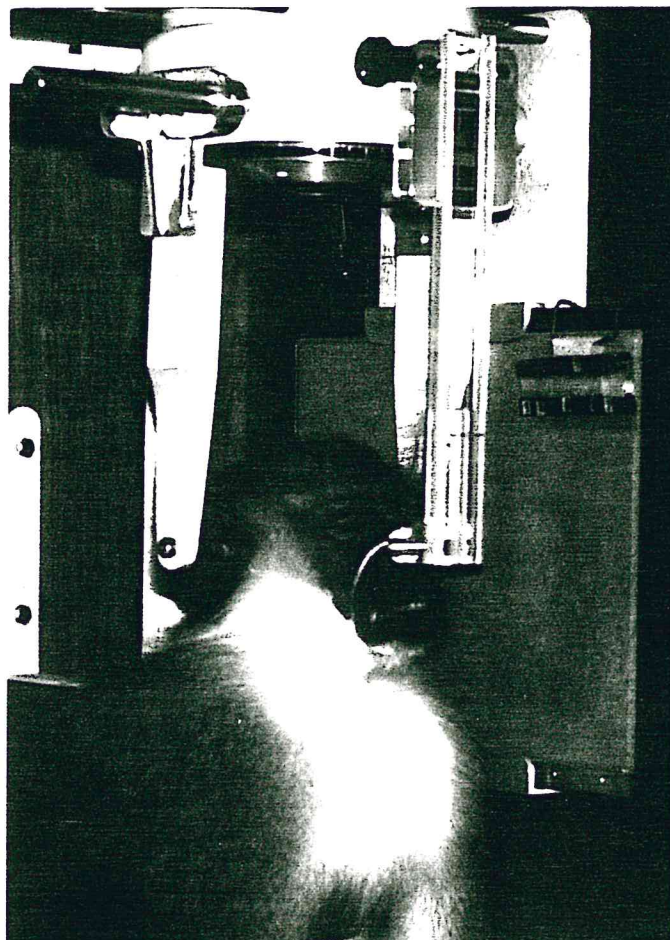
Figure 2. Anesthesized vervet monkey in position for
taking lateral cephalometric roentgenogram.
Cassette in position for lateral roentgeno-
gram.
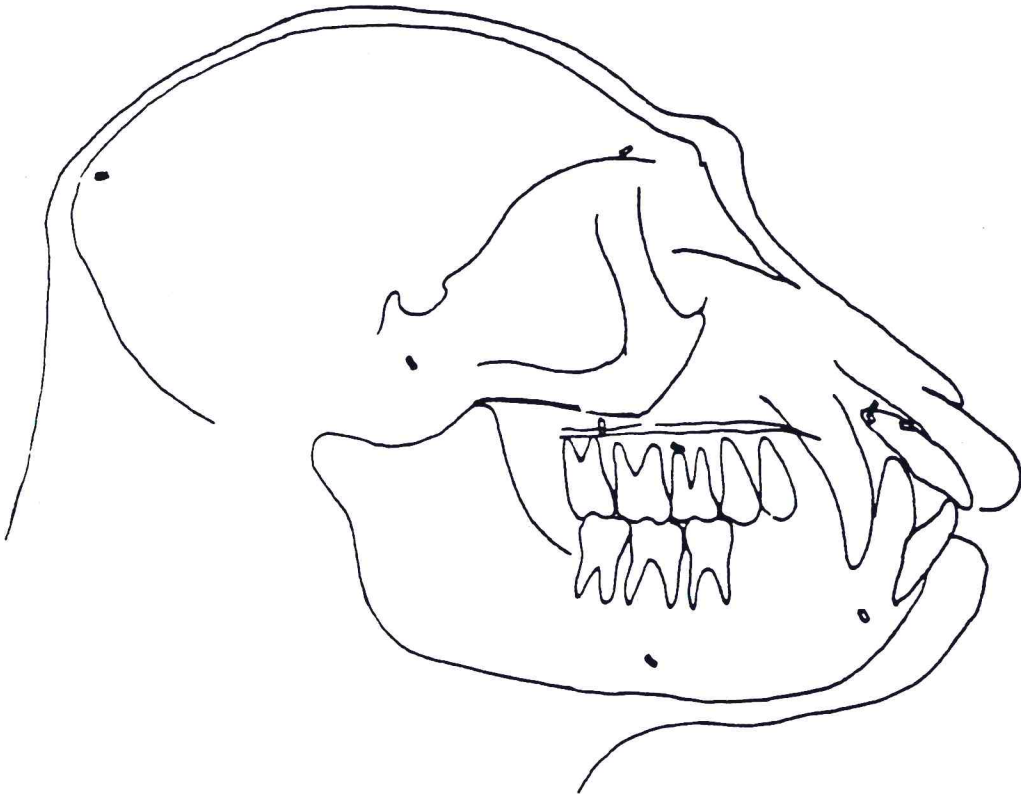
Figure 3. Tracing of the lateral cephalometric roentgenogram
indicating anatomical structure and position of
implants.

1985). These two measurements and a "mechanical efficiency index" were used to characterize the features in the masticatory system. These measures, described below, are illustrated in Figure 4.

Lever arm length represents the distance from the line of action of the masticatory muscle to the articular eminence of the temporomandibular joint. Since the vervet monkey does not have a clear articular eminence, condylion, the most superior point on the condylar surface, was used. The inferior most border of the Zygomaticomaxillary suture was used to indicate the most anterior possible line of action of the masseter muscle.

Load arm length represents the distance from the condylion to selected points on the maxillary occlusal surface; i.e., to the most occlusal point of the incisal edge of the maxillary central incisor, to the approximate center of the maxillary first permanent molar, to the second deciduous second molar, and to the most posterior wear point of the tooth row.

A mechanical efficiency index was obtained by comparing average masticatory lever arm and load arm lengths according to the formula: lever arm length/load arm length x 100, a procedure previously established by Oyen et al. (1979).

Part II: Magnetic Resonance Imaging data gathering procedures

Magnetic resonance imaging was performed on a Picker 0.5T (Tesla), VISTA 2055 MR imager (Figure 5), using standard software and a small receiver coil. A brief description of these procedures is provided below; a more detailed description is given in the Appendix.
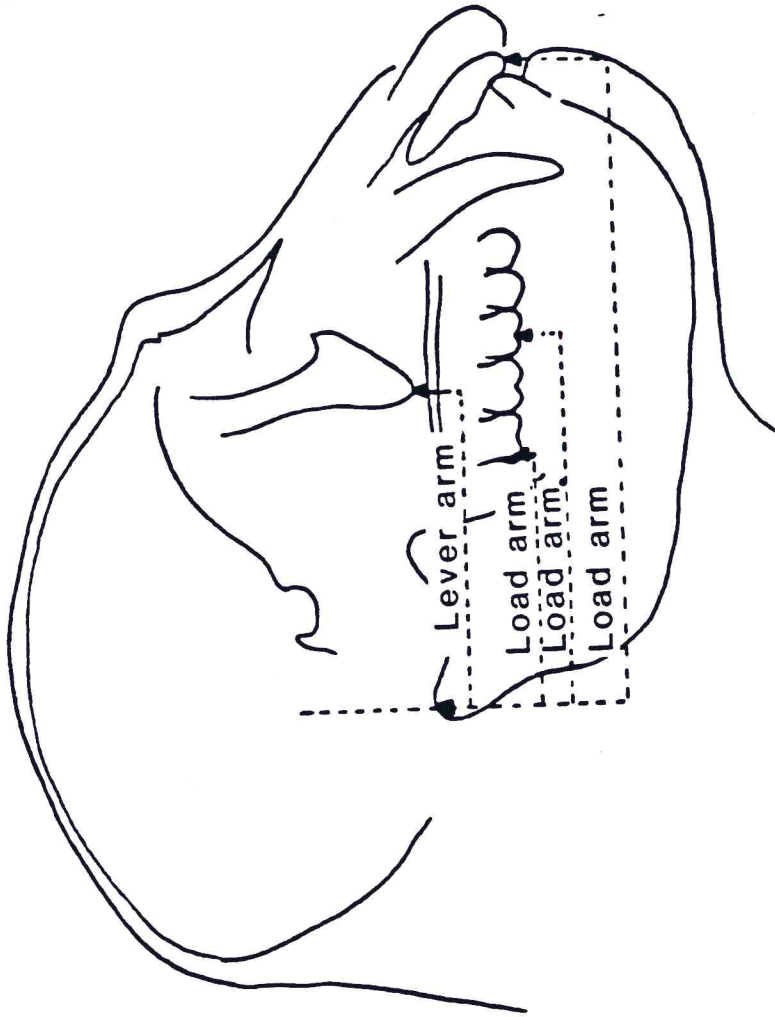
Figure 4. Lateral cephalometric roentgenogram indicating the measurements of lever arm and load arm length.
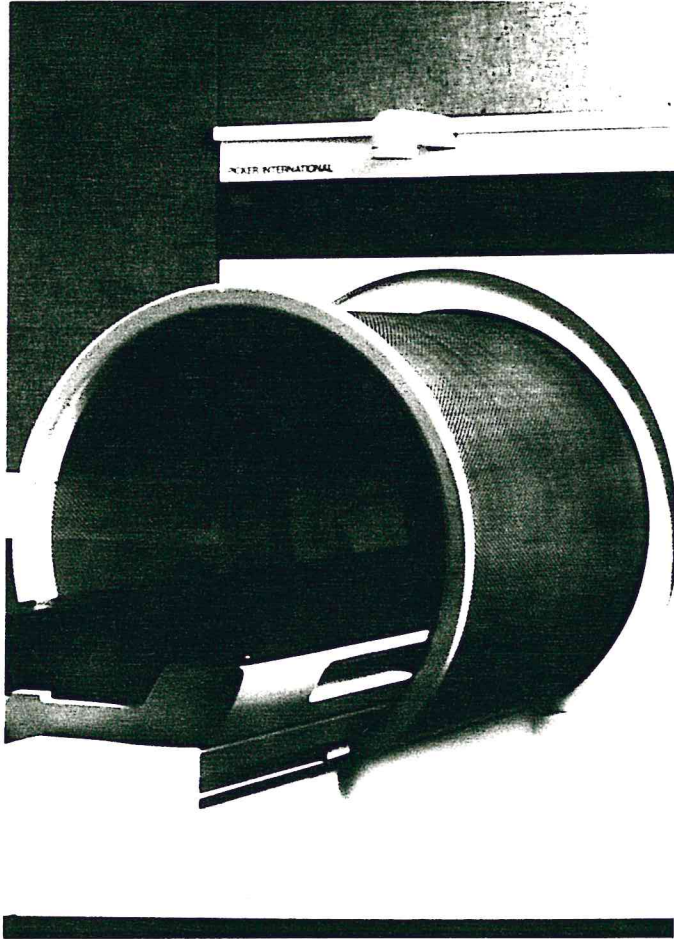
Figure 5.   VISTA magnetic resonance imager.

All the Magnetic resonance imaging data were obtained using instruments maintained at the Corporate Headquarters of Picker International. These procedures required transporting each monkey, lightly sedated, from the Case Western Reserve University animal facility. At the imaging facilities, the animal was fully anesthetized before scanning.

All scans were made with the monkey's head in a symmetrical orientation (median plane at a right angle to scan plane). A laser positioning system was used to position the head along the Frankfort and Suborbital horizontal plane. (This system utilizes three orthogonal laser beams to achieve localization which is accurate to 1mm depending on the anatomical reference point). In order to improve image quality given the relatively small craniofacial volume of each monkey, a small "joint" coil (Figure 6) was used as a receiver. Use of this smaller receiver coil enhances image quality by decreasing the distance and maximizing the signal reception. The small coil (multiple loops of wire designed to produce the magnetic field from current flowing through the wire or to detect the changing magnetic field by voltage induced in the wire) was used by wrapping it around the monkey's head. The major advantage of using this coil is for image quality improvement for small volume. This coil was used as a receiver that maximizes signal reception by closely conforming to the monkey's head.

A pilot reference image was initially acquired (Figure 7). Once a reference image is selected, the operator may prescribe the
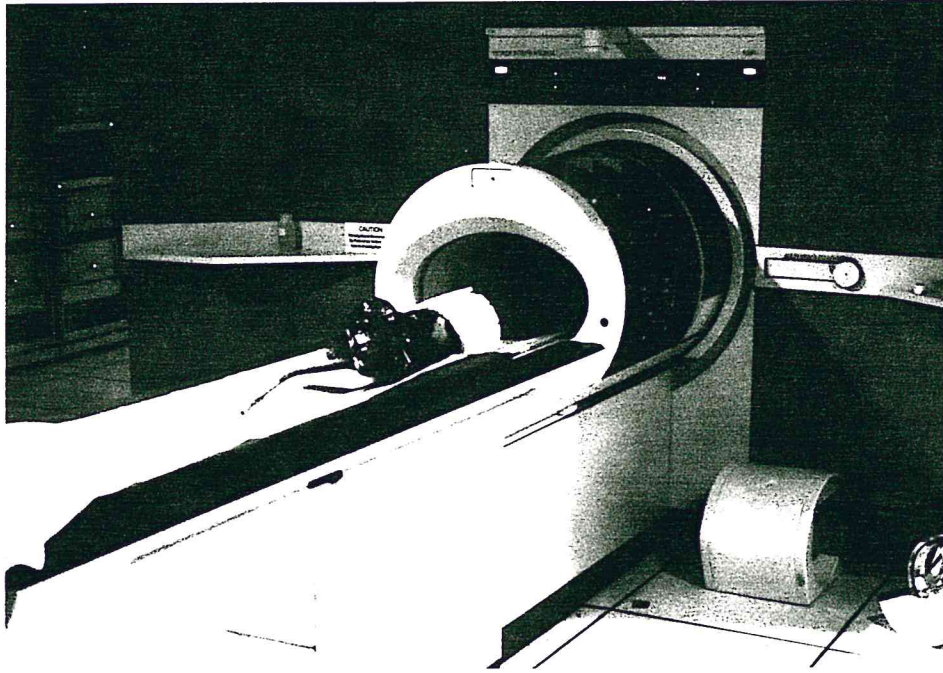
Figure 6.   VISTA Imager with an anesthetized monkey
in place. The monkey's head is enclosed
in a small "joint" coil.
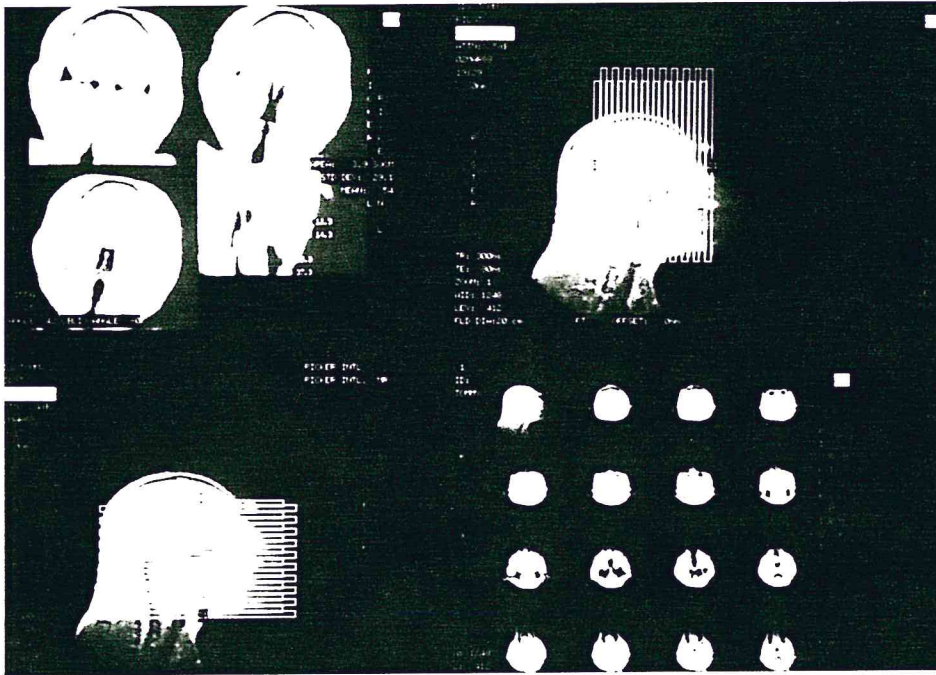
Figure 7. A composite of four Magnetic Resonance Images

Upper left: Instant oblique reconstruction
               from the coronal section.

Upper right: Sagittal pilot scan showing position
               of each slice in the coronal plane.

Lower left: Sagittal pilot scan showing position
               of each slice in the transverse plane.

Lower right: All images of a given scan sequence
               shown in the transverse section.

position of the target acquisition by pressing the reference lines anywhere on the image. The positions of these lines/slices will be automatically loaded into the system. Field echo images were obtained with the FESUM protocol (the signal from water and fat in any tissue is additive) and 90 degree flip angles (amount of rotation of the macroscopic magnetization vector produced by an radiofrequency pulse, with respect to the direction of the static magnetic field).

The orientation of the scanning planes was determined on the basis of a sagittal pilot 20mm thick (Figure 7). The positioning of the slice was determined by adjustment of a grid showing the position of each slice in the scan. This positioning procedure is accurate to ±1 pixel (±2mm).

In each monkey, sets of images were acquired in the coronal and transverse planes. The rationale for using these two orientations was due to the fact that their sections represent the largest anatomical cross-sectional area of the masticatory muscles. The images were obtained using the FESUM sequence, TE (echo time) = 12 milliseconds, TR (repetition time) = 800 milliseconds, 20 contiguous slices of 3.5mm each, 20cm field of view, 2 repetitions and 256 views. These parameters were selected to optimize resolution, contrast and signal-to-noise ratio. Total scan time was twenty minutes for each scan including set up, scanning, initial data reconstruction and cine viewing. All data were stored in the computer system. The images were archived onto magnetic tape, and hard copies were selectively obtained on a multi-format camera. The

images were photographed by a 3M laser camera with 3M laser imaging film, and hard copies were obtained after film processing in a Kodak processor.

The first magnetic resonance imaging data collection was performed in January of 1987, with a second data collection in January of 1988. Seventy-eight magnetic resonance imaging scans were completed and stored in the computer. Once primary magnetic resonance data were collected, these data were treated according to the following techniques. Instant oblique reconstruction (IOR) software is a postscan-processing capability which allows the reconstruction of previously acquired scan data at any angle oblique to the original image plane. This procedure can be used to automatically reconstruct the transverse and coronal scan data into oblique sections so that the slices are taken perpendicular or parallel to the long axis of the muscle. The line of action of each muscle, medial pterygoid and masseter, was determined in coronal planes (Figure 8) by placing an electronic axis as close as possible at a right angle to the mean fiber direction of the muscle. The maximum thickness of the muscle was selected by the operator, then instant oblique reconstruction was obtained at the maximum cross-sectional area of each muscle. For the temporalis muscle, where the line of action is perpendicular to the transverse plane (Figure 9), the cross-sectionsl area was obtained by direct measurement at the area above the zygomatic arch but below the plane
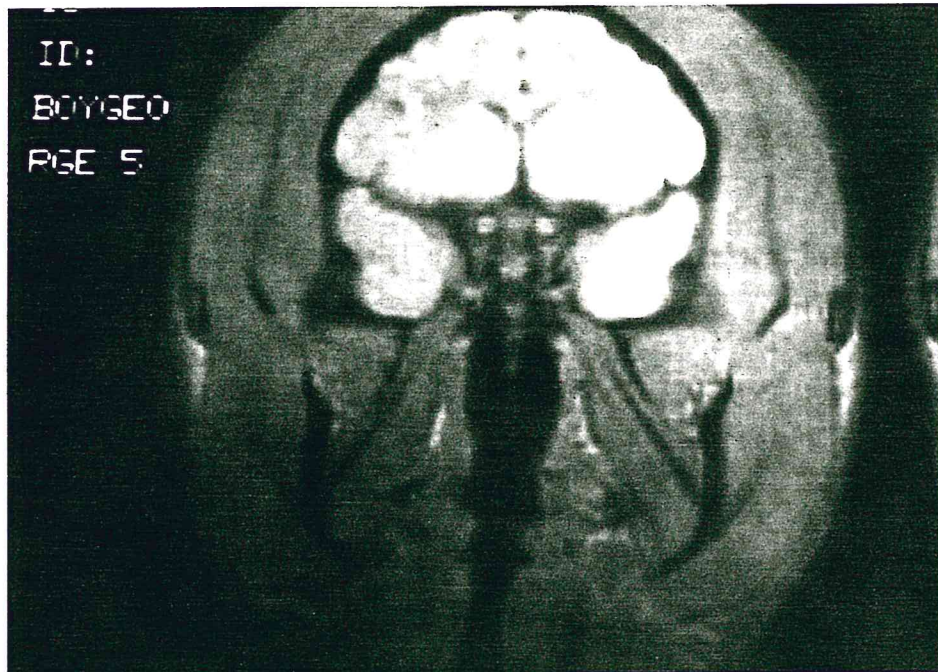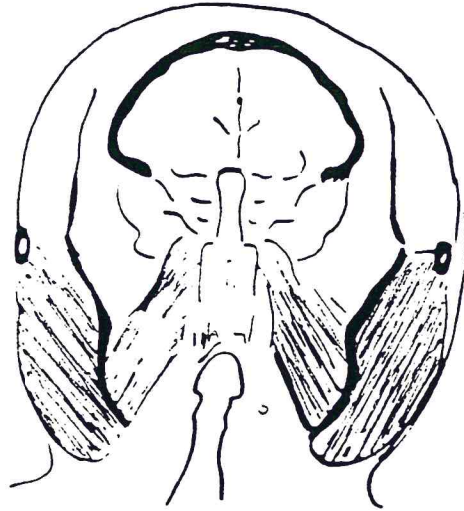
Figure 6. Coronal section of head with masseter and medial pterygoid muscles indicated.
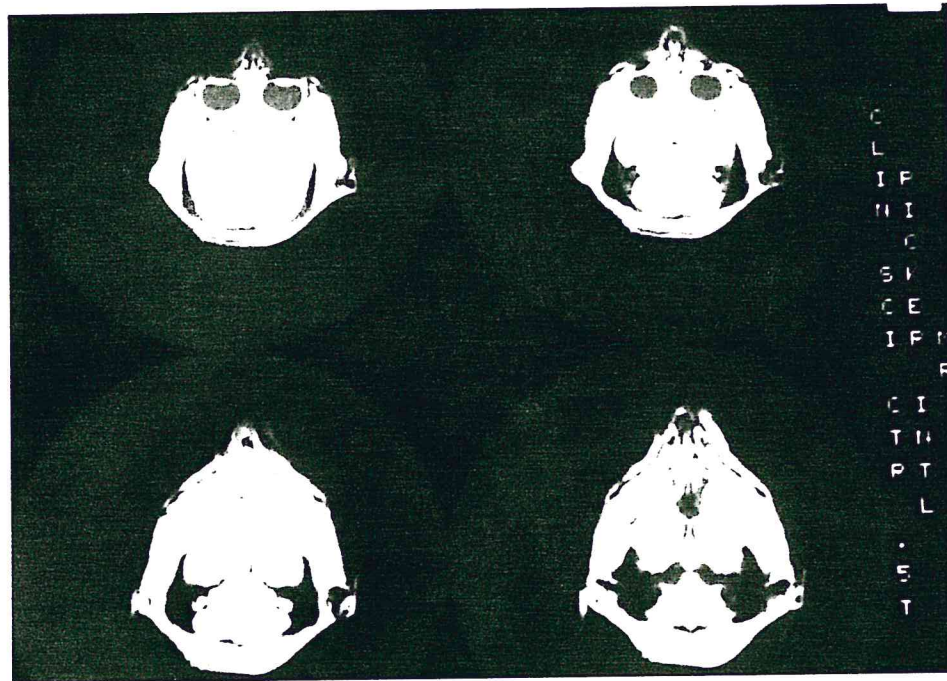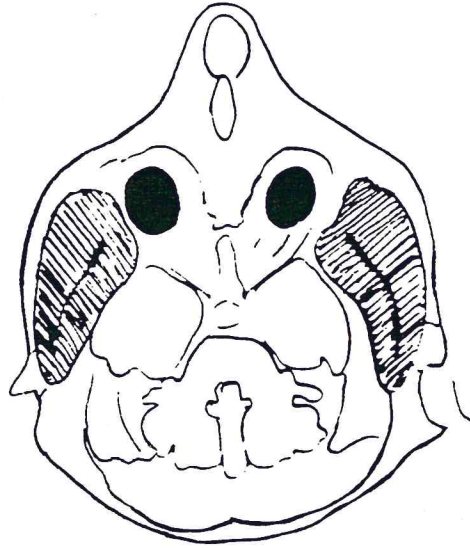
Figure 9. Transverse section of head with temporalis muscle
            indicated.

of the orbital floor of a cross-section that showed no evidence of the medial pterygoid muscle.

Based on the images from instant oblique reconstruction, area, linear and angular measurements of the elevator muscles were made using standard software and were read directly from the computer screen. The computer generated the following measurements (Figure 10):

1. Linear distance of the maximum cross-sectional of the muscles.

2. The angles of the long axis of the muscles relative to the horizontal plane.

3. The maximum cross-sectional area of the muscle in square centimeters.

Calibration and measurement error

The magnetic resonance scan parameters used in this study are carefully calibrated so that images produced using a 20 cm imaging field of view and a 512^2 pixel matrix on the image display will produce images with a spatial resolution of 10 line pairs per cm (.55mm) with ±1 pixel where 1 pixel =.33mm for the scan parameters used in this study. Geometric distortion of the image is maintained at less than 3% of the field of view by quality assurance and quality control calibration procedures.

To control for measurement errors, each reconstruction was measured three times before the mean value and standard deviation were obtained. The individual measurement error was calculated at 4%.
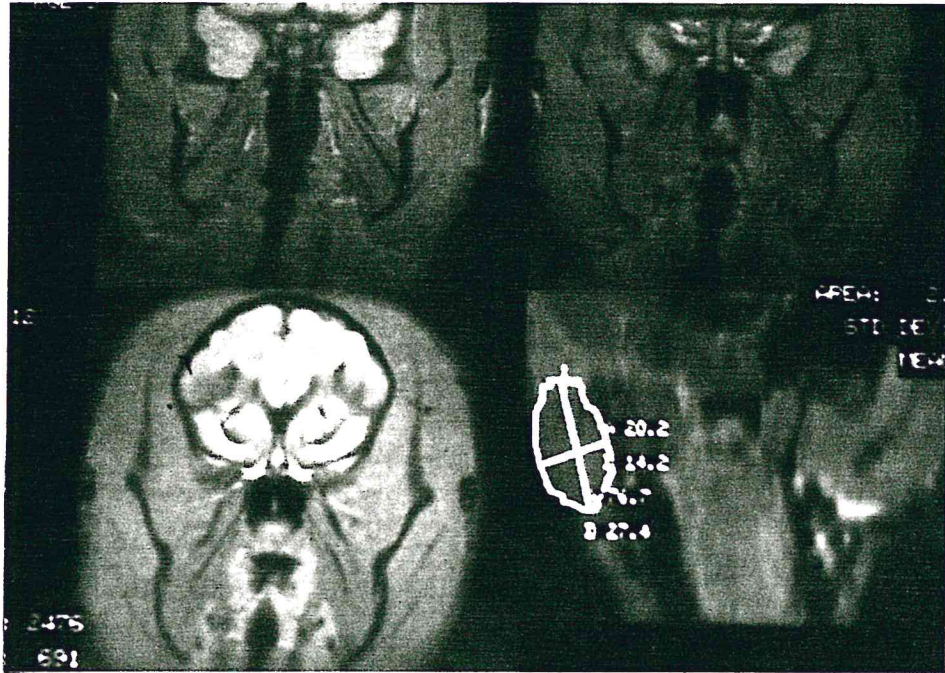
Figure 10. Coronal section of head with instant oblique
reconstruction in lower right figure.

In order to check the accuracy of imaging data, the range of variation in measurements was crossed-checked by using phantom scans (Figure 11). A phantom was used for quality assurance and calibration of the images since it was constant throughout the experiment. The phantom was scanned _at 0.5 T system and showed a resolving power of 8.2 linepair/cm. The same sequence parameters were obtained in both the phantom and monkey scans.

In addition, direct measurement of the muscles of interest (temporalis and masseter muscles) was performed in anesthetized monkeys in order to compare maximum thickness of a cross-sectional area of the muscle determined from magnetic resonance imaging data with direct measurements which were obtained in the following manner. A long needle was pierced into the estimated deepest muscle fiber. The maximum distance was chosen to be the estimated thickness of the muscle. The temporalis muscle landmark was estimated by palpating the upper border of the zygomatic process, and the needle was inserted perpendicular to and lightly touching the zygomatic arch, and the depth of the penetration was marked at the needle. The needle was then extracted and the penetration depth measured. For the masseter muscle, the landmark was estimated by the deepest point between the half distance from zygomatic process to the angle of mandible. The procedures were repeated until obtaining the maximum distance.

Part III: Bite Force Measurements.

Masticatory bite force was measured by bite force transducer techniques. The rationale for using this procedure is derived from a
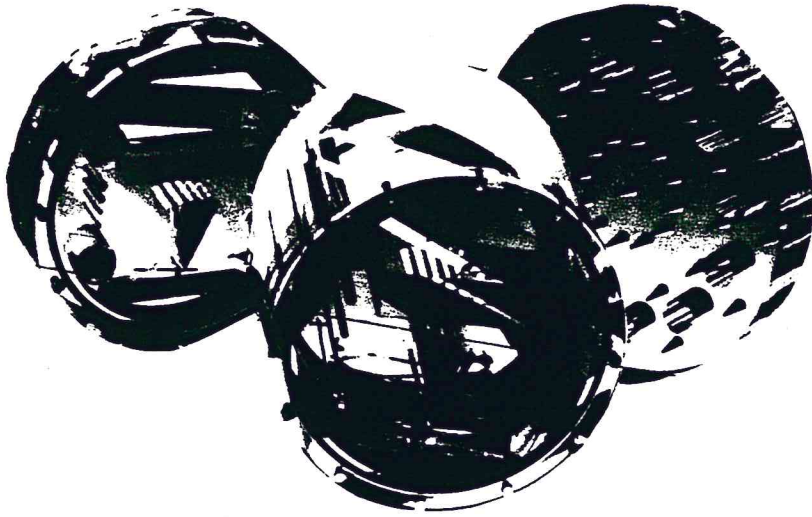
Figure 11. (Upper) Phantom

(Lower) Phantom Image

growing body of evidence which links magnitudes of bone strain in parts of the skull with levels of force associated with mastication (Weijs and Dejogh, 1977; Hylander, 1979; Bouvier and Hylander, 1981). To achieve maximum bite force (tetanic contraction of the jaw elevator muscles), instrumentation and procedures worked out of Dechow and Carlson (1983) were used. Briefly, these procedures were as follows: a monkey was anesthetized, and unipolar platinum needle electrodes were inserted into the right and left masseter and temporalis muscles thorough the skin. The electrodes were then attached to a galvanic stimulator. Three levels of stimulation, 60,70 and 80 volts (all at 0.8 milliseconds, 60 hertz), were employed during dental loading. Each level of stimulation was applied for 1-2 seconds, insuring that full tetany of the jaw elevator muscles was obtained. To measure the force generated by contraction of the muscles, a bite force potentiometer (Figure 12) was placed between the upper and lower jaws at selected points along the tooth row, eg. at the incisors, first molars, second molars, etc.. Through the use of a bite force potentiometer, reliable, reproducible quantitative data establishing maximum bite force levels was generated (Dechow and Carlson, 1983; Oyen, 1987).

Data collection errors attributable to sensor or recording errors during bite force recording sessions were guarded against in several ways. The bite force sensor was routinely calibrated and tested by applying known amounts of force to the sensor. To minimize the likelihood of muscle fatigue occurring during a recording
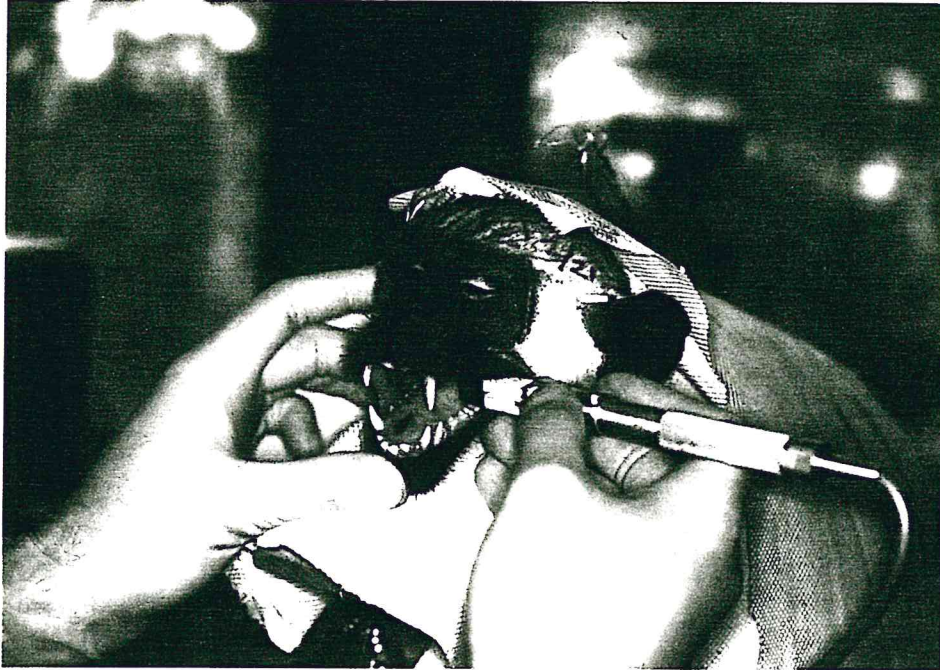
Figure 12. Bite force potentiometer placed between upper
and lower jaw at selected point along the tooth row.
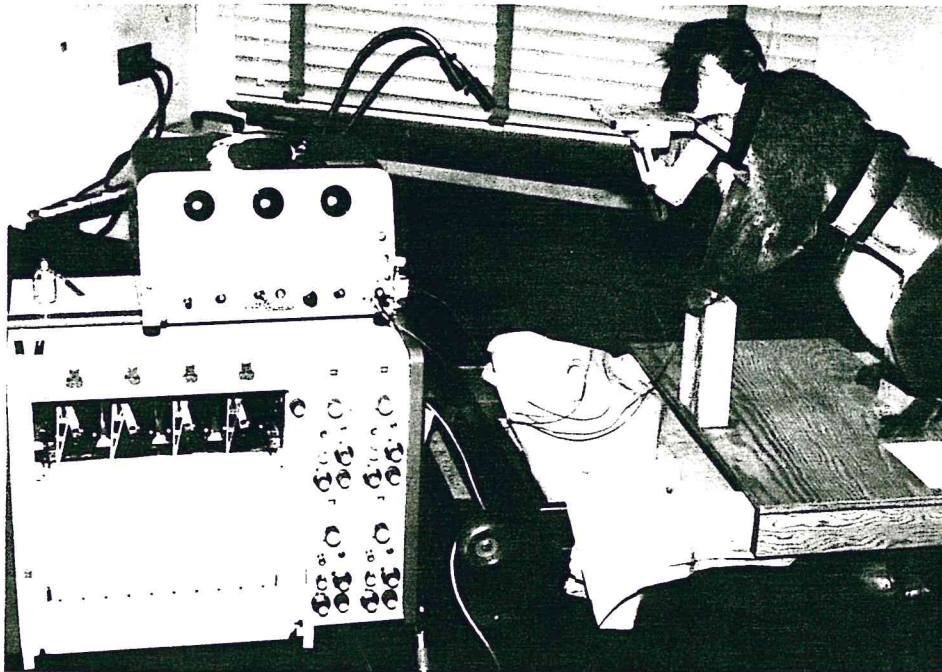
Figure 13. Anesthetized monkey in position for bite force
measurement procedure.

session, each bite point along the tooth row was sampled once, working from posterior to anterior, with the electrical stimulus limited to a maximum duration of 1-2 seconds at each bite point. The monkey was then allowed to rest for several minutes before the bite force/stimulation procedure was repeated (Figure 13). When values obtained in the two instances were within ten percent of each other, the highest value was used. If the values were separated by more than ten percent, the test was repeated at that bite point, and the highest value used in subsequent analyses.

Part IV: Data Analysis

Descriptive statistics of the data were calculated in order to provide clearer insights into in vivo changes in masticatory biomechanics, to summarize age-related changes in the variables, and to establish correlations between structural morphology and function. Descriptive statistics were calculated to characterize relationships among the variables, with hard and soft diet treated separately, as well as pooled. Relationships among variables such as cross-sectional area of the jaw elevator muscles, bite force, selected cephalometric dimension, body weight and estimated chronological age were assessed using correlation analyses.

RESULTS

Quantitative Analyses

The mean values of cross-sectional areas of the jaw elevator muscles of fifteen monkeys obtained from magnetic resonance imaging measurements are shown in TABLE II.

The temporalis muscle has the largest cross-sectional area, and the cross-sectional area of the masseter is larger than the cross-sectional area of the medial pterygoid muscle.

The relationships among the cross-sectional areas in the three elevator muscles are shown in Figure 14 and TABLE III. There appears to be a highly significant positive correlation between the cross-sectional area of the masseter and the cross-sectional area of the medial pterygoid muscle ($r^2 = 0.67$). The correlation of the cross-sectional area of the temporalis and the cross-sectional area of the medial pterygoid ($r^2 = 0.25$) is lower than the correlation between the cross-sectional area of temporalis and the cross-sectional area of the masseter muscles ($r^2 = 0.39$, $p<.0005$).

In Figure 15 and TABLE IV a significant linear relation between the cross-sectional area of the muscle versus body weight can be observed.

The correlation coefficients for the cross-sectional areas of the temporalis, medial pterygoid and masseter muscles versus body weight are 0.51, 0.62 and 0.58 respectively.

Using a two-tailed test of significance at the .05 level,

there is no evidence of linear relation between the cross-sectional area of the muscles versus the estimated ages (Figure 16 and TABLE V).

Relative changes in cross-sectional areas of the jaw elevators muscles are shown in TABLE V. These relative changes were provided by the five youngest monkeys in our sample. The time interval is approximately one year, falling between the initial and final magnetic resonance data collections.

The cross-sectional areas of the elevator muscles versus the bite force capabilities is shown in Figure 17 and TABLE VI. A significant positive correlation for the medial pterygoid and masseter muscle is shown. However, the temporalis muscle shows a positive (but statistically insignificant) correlation.

Dimensions of the masticatory system, that is, lever arm, load arm length, mechanical efficiency index and status of dental development are presented in TABLE VII.

Figure 18 and TABLE VIII show no linear correlation between cross-sectional areas of the jaw elevator muscles and the mechanical efficiency index at incisor bite point. Low significant correlation is found between the mechanical efficiency index at molar bite point and the cross-sectional areas of masseter and medial pterygoid muscles.

In Figure 19, all animals show highly significant positive linear relationships of the lever arm and load arm length at incisor, first permanent molar and posterior wear point of the tooth row

(TABLE IX). A significant positive correlation is found between lever arm and the cross-sectional area of the masseter and the cross-sectional area of the temporalis muscle (Figure 20, Figure 21 and TABLE X).

The relationship between the mechanical efficiency index and age in the same individual monkey is shown in Figure 22 and TABLE XI. The mechanical efficiency index at incisor bite point shows no evidence of a linear relation between age and the mechanical efficiency. The slope is very low (-.005), indicating that the curve is almost flat. At the first molar, a downward slope is seen, indicating that the mechanical efficiency index decreases with time. The index at the posterior wear point shows an oscilating pattern and tends to reach a plateau at about 50 months. Each peak represents a given occlusal phase.

The relationships between the mechanical efficiency index at incisor bite point and body weight (Figure 23 and TABLE XII) show no evidence of a linear relation. At the first molar, a downward slope is seen, indicating that the mechanical efficiency index decreases as the monkey increases in weight. The index at the posterior wear point shows an oscilating pattern and tends to reach the plateau at about 5.5 kg.

The relationship between age and the maximum bite force capabilities is depicted in TABLE XIII. For an individual animal, the relationship between age and the forces at incisor, first molar, or second molar bite points shows a significant positive correlation

(Figure 24). The hard diet group has higher correlation to age than the soft diet group (TABLE XIII). The relationship between the maximum bite force capability and body weight (Figure 25 and TABLE XIV) also shows a positive linear correlation. The hard diet group also has a higher correlation between bite force and body weight than the soft diet group.

In Figure 26 and TABLE XV, the relationship between the maximum bite force capabilities at incisor and the mechanical efficiency index at incisor shows a statistically insignificant correlation.

The relationship between the bite force at first permanent molar and the mechanical efficiency index at molar bite point (Figure 27 and TABLE XV) shows a downward slope, indicating a significant inverse linear trend in which the bite force increases, and the mechanical efficiency index decreases.

The relationships between mechanical efficiency index, the bite force and the cross-sectional areas of the masseter muscle vs estimated age are shown in Figure 28. According to these results, while the mechanical efficiency index decreases, bite force increases, and cross-sectional area of the masseter muscle increases slightly, especially between 43-45 months, before reaching a plateau at about 45 months.

TABLE II.

MEAN AND STANDARD DEVIATION OF THE CROSS-SECTIONAL AREAS OF
THE JAW EVELATOR MUSCLES FROM MAGNETIC RESONANCE IMAGING.

Cross-sectional Area (CM^2)	M. Pterygoid	Masseter	Temporalis
Mean (x)	2.20	3.07	6.65
SD	0.59	0.81	1.80
Sample (n)	27.00	27.00	29.00
Soft Diet			
Mean (x)	2.34	3.40	7.50
SD	0.74	1.13	2.12
Sample (n)	9.00	9.00	10.00
Hard Diet			
Mean (x)	2.07	2.91	6.21
SD	0.54	0.53	1.42
Sample (n)	18.00	18.00	19.00
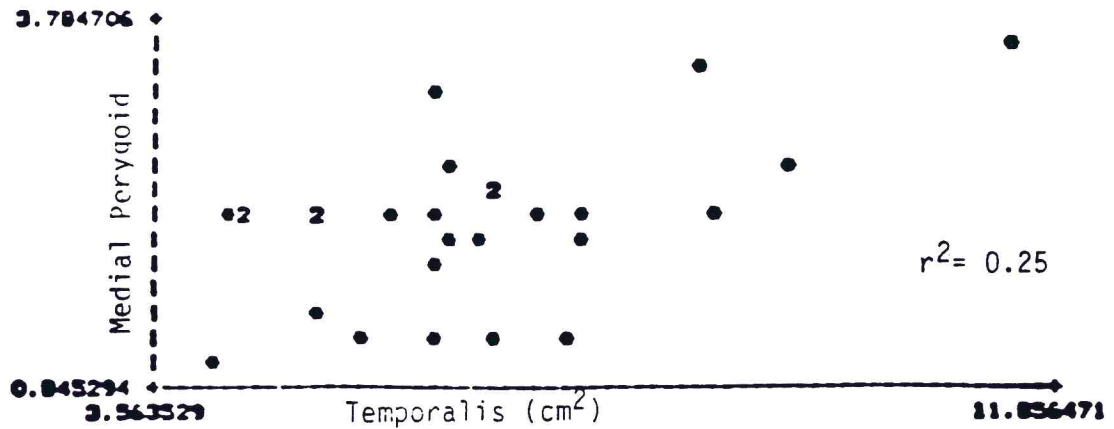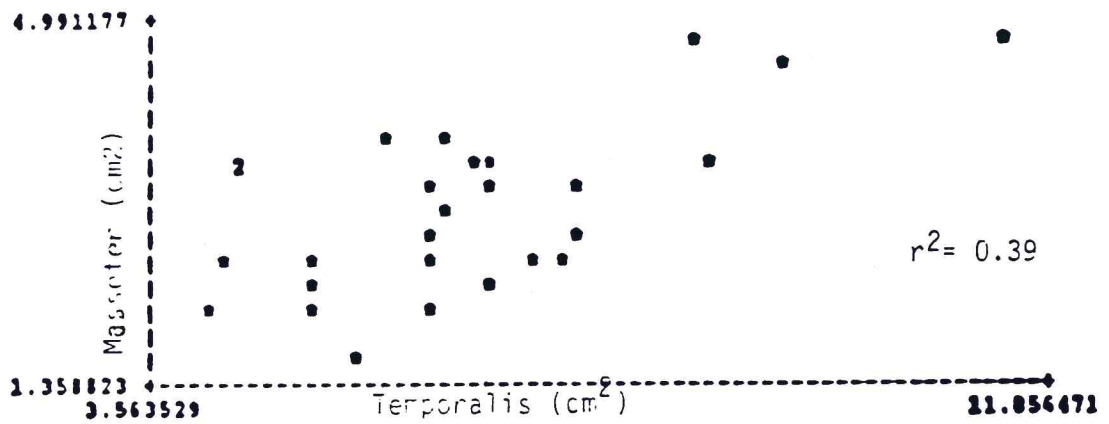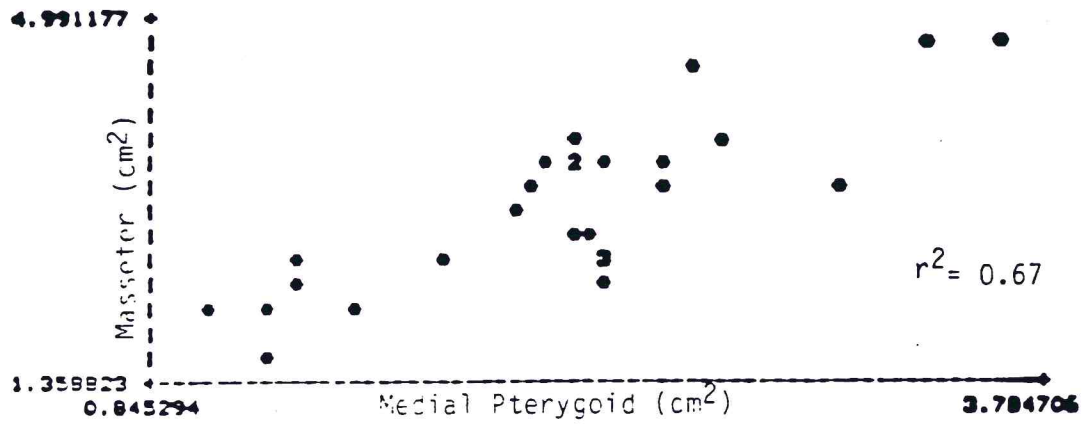
Figure 14. Scatter plots comparing cross-sectional areas of the jaw elevator muscles (cm²).

TABLE III.

RELATIONSHIPS AMONG THE CROSS-SECTIONAL AREAS OF
MASSETER, MEDIAL PTERYGOID AND TEMPORALIS MUSCLES.

Cross-sectional Area (cm^2)	M. Pterygoid -Masseter	Masseter -Temporalis	Temporalis -M.Pterygoid
Correlation (r^2)	0.67	0.39	0.25
T-value	7.09*	3.97*	2.86*
Slope	1.06	0.30	0.18
Intercept	0.77	1.15	0.97
Sample (n)	26.00	26.00	26.00

*Indicates significant correlation at .005 level.

TABLE IV.

RELATIONSHIPS BETWEEN THE CROSS-SECTIONAL AREAS
OF THE JAW ELEVATOR MUSCLES AND BODY WEIGHT.

Cross-sectional Area and Body Weight (kg)	M. Pterygoid	Masseter	Temporalis
Sample (n)			
Soft diet	8.00	8.00	9.00
Hard diet	17.00	17.00	18.00
TOTAL	26.00	26.00	26.00
Correlation (r^2)			
Soft diet	0.69	0.85	0.87
Hard diet	0.57	0.41	0.27
TOTAL	0.62	0.58	0.51
Slope			
Soft diet	0.69	1.17	2.32
Hard diet	0.46	0.38	0.81
TOTAL	0.54	0.67	1.42
T-value			
Soft diet	4.04*	6.28*	7.31*
Hard diet	4.58*	3.36*	2.48*
TOTAL	6.40*	5.83*	5.34*

*This statistical analysis used three independent models: soft diet, hard diet and total (all monkeys) in which each model used one degree of freedom. The sum of the sampled animals can, therefore, be less than the total because it involves two degree of freedom.
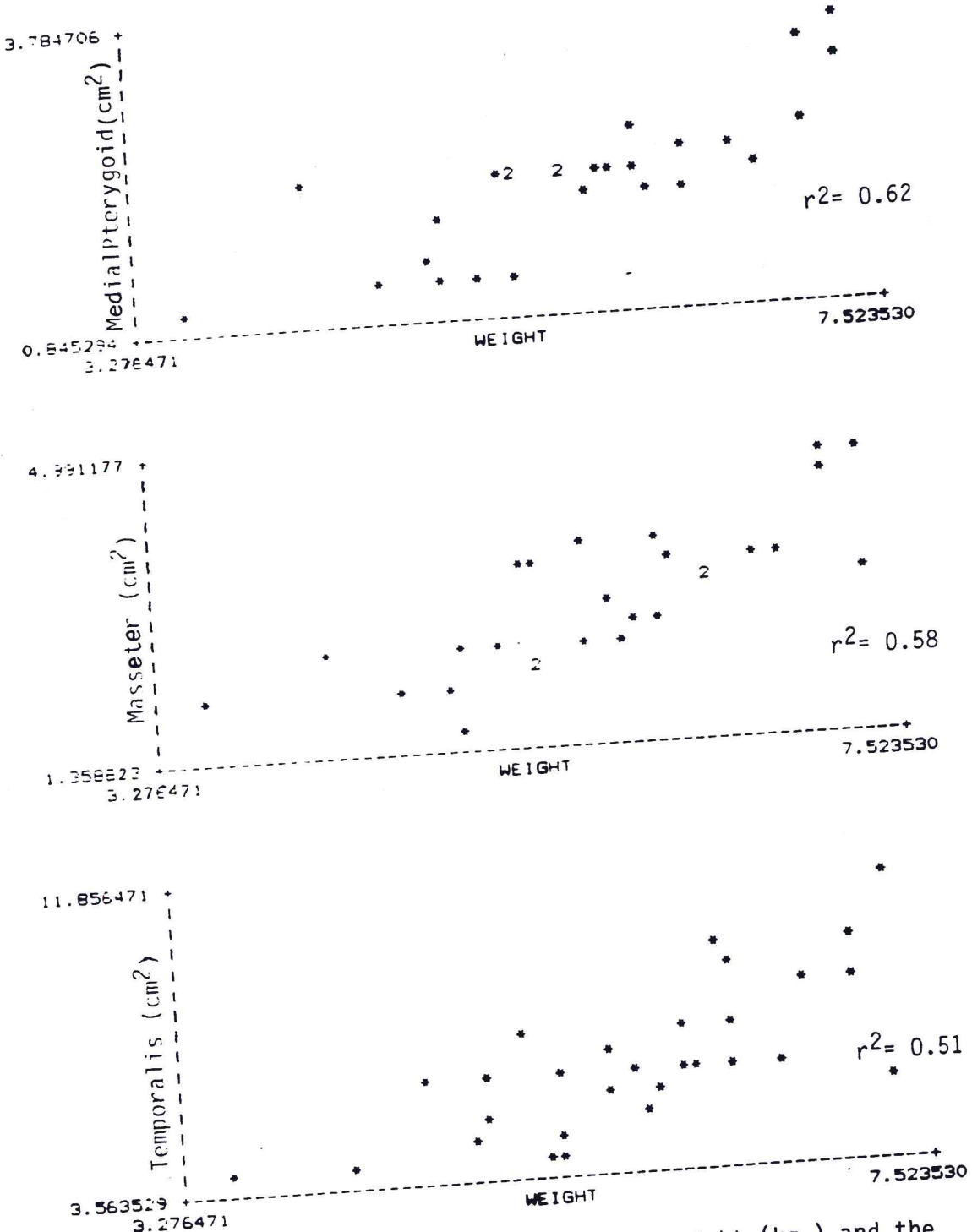
Figure 15. Scatter plots comparing the body weight (kg.) and the cross-sectional areas of the jaw elevator muscles (cm^2).

TABLE V.

RELATIONSHIPS BETWEEN THE CROSS-SECTIONAL AREAS OF JAW ELEVATOR MUSCLES AND ESTIMATED CHRONOLOGICAL AGE.

Cross-sectional Area (cm^2) and Age (mos.)	M. Pterygoid	Masseter	Temporalis
Sample (n)			
Soft diet	8.00	8.00	9.00
Hard diet	17.00	17.00	18.00
TOTAL	26.00	26.00	26.00
Correlation (r^2)			
Soft diet	0.59	0.67	0.52
Hard diet	0.85	0.21	0.05
TOTAL	0.16	0.23	0.09
Slope			
Soft diet	0.08	0.13	0.21
Hard diet	0.02	0.03	0.03
TOTAL	0.03	0.05	0.06
T-value			
Soft diet	3.16	3.76*	2.95
Hard diet	1.22	2.04	0.95
TOTAL	2.18	2.75	1.65
Total different			
sample (n)	11.00	12.00	13.00
Correlation (r^2)	0.03	0.02	0.10
Slope	0.03	0.05	-0.17
T-value	0.52	0.48	-1.14

Relative changes in cross-sectional areas of the jaw elevator muscles. Calculated by comparing the difference in values between 1987 and 1988 data gathered in the five youngest animals.

Animal Number	M. Pterygoid	Masseter	Temporalis
6	0.30	0.09	0.15
11	0.18	0.31	0.08
13	0.27	0.49	0.06
15	0.53	0.20	0.01
16	0.03	0.02	0.21
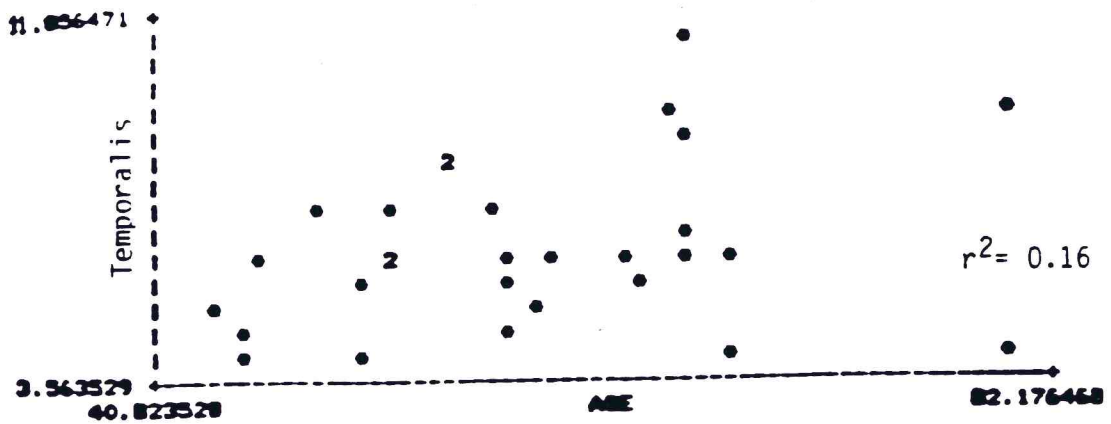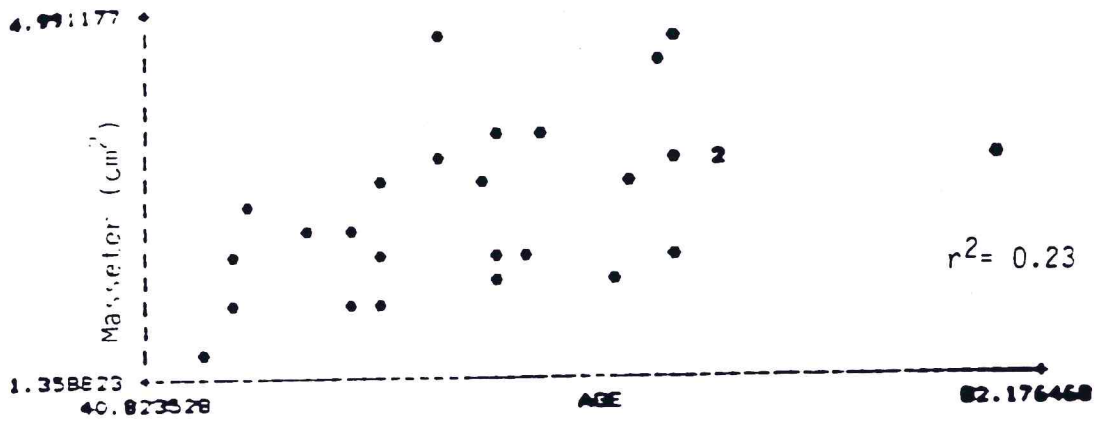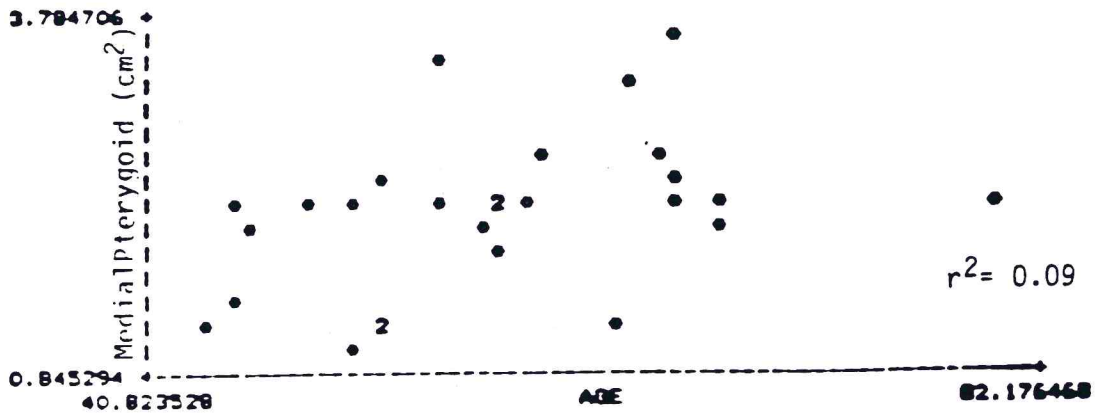
Figure 16. Scatter plots comparing cross-sectional areas of the jaw elevator muscles and chronological age.

TABLE VI.

RELATIONSHIPS BETWEEN THE CROSS-SECTIONAL AREAS OF THE JAW ELEVATOR
MUSCLES AND BITE FORCE CAPABILITIES AT INCISOR.

Cross-sectional Area (cm^2) & Bite Force at Incisor (kg)	M. Pterygoid	Masseter	Temporalis
Sample (n)			
Soft diet	8.00	8.00	8.00
Hard diet	17.00	17.00	17.00
TOTAL	26.00	26.00	26.00
Correlation (r^2)			
Soft diet	0.53	0.30	0.58
Hard diet	0.38	0.63	0.12
TOTAL	0.30	0.24	0.09
Slope			
Soft diet	0.15	0.17	0.46
Hard diet	0.06	0.07	0.07
TOTAL	0.07	0.08	0.09
T-value			
Soft diet	2.82*	1.75	3.15*
Hard diet	3.14*	5.20*	1.50
TOTAL	3.24*	2.79*	1.61
Total different			
Sample (n)	11.00	12.00	13.00
Correlation (r^2)	0.04	0.33	0.01
Slope	-0.02	-0.10	0.03
T-value	-0.67	-2.34*	0.39

TABLE VI. (cont'd)

RELATIONSHIPS BETWEEN THE CROSS-SECTIONAL AREAS OF THE JAW ELEVATOR
MUSCLES AND BITE FORCE CAPABILITIES AT MOLAR.

Cross-sectional Area (cm^2) & Bite Force at Molar (kg)	M. Pterygoid	Masseter	Temporalis
Sample (n)			
Soft diet	8.00	8.00	8.00
Hard diet	17.00	17.00	17.00
TOTAL	26.00	26.00	26.00
Correlation (r^2)			
Soft diet	0.53	0.22	0.45
Hard diet	0.34	0.53	0.16
TOTAL	0.35	0.24	0.17
Slope			
Soft diet	0.07	0.06	0.18
Hard diet	0.03	0.04	0.04
TOTAL	0.04	0.04	0.08
T-value			
Soft diet	2.79*	1.40	2.41*
Hard diet	2.87*	4.21*	1.72*
TOTAL	3.67*	2.86*	2.23*
Total different			
Sample (n)	11.00	12.00	13.00
Correlation (r^2)	0.13	0.29	0.05
Slope	-0.02	-0.04	0.03
T-value	-1.19	-2.12	0.81
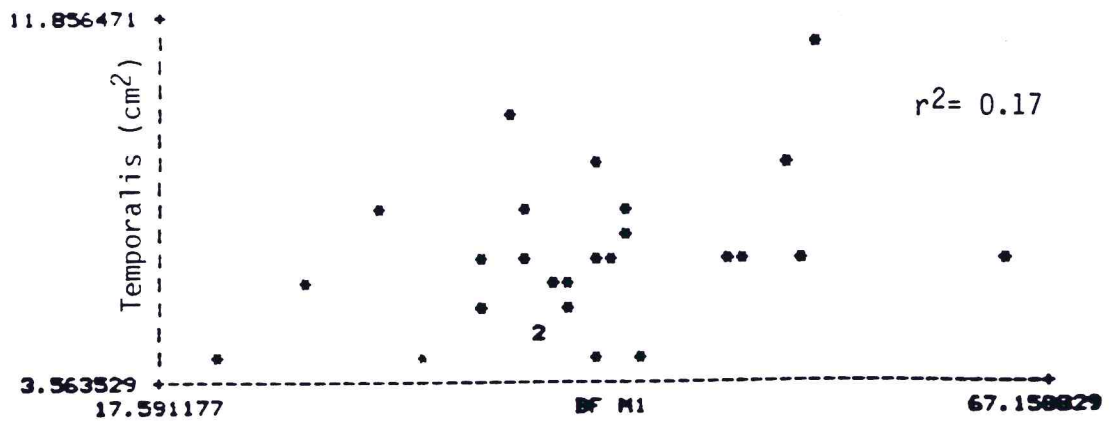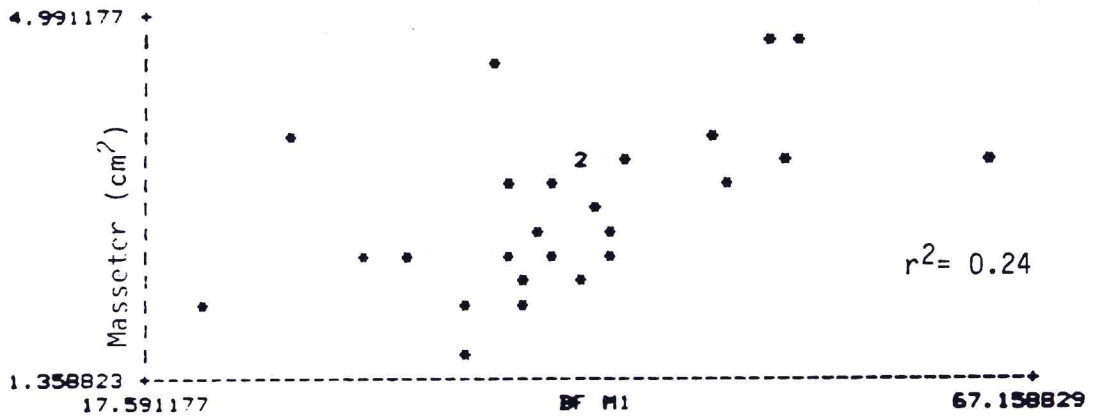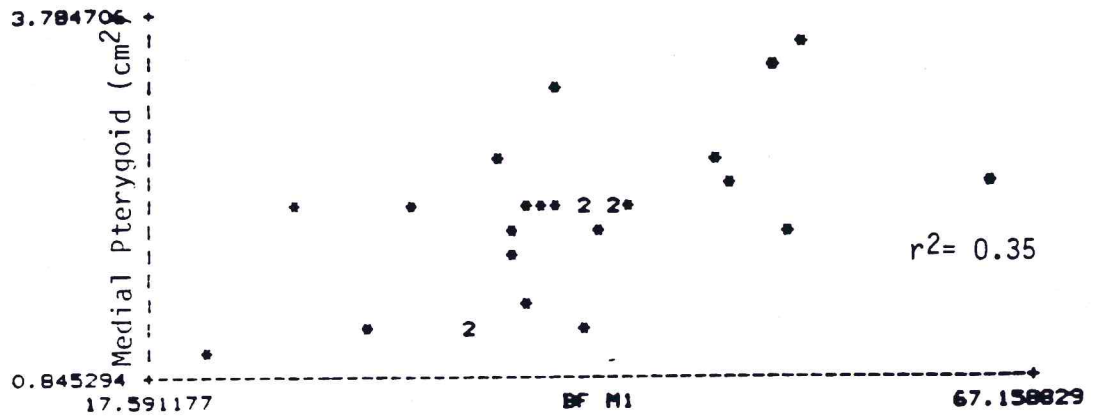
Figure 17. Scatter plots comparing cross-sectional areas of the jaw elevator muscles and the bite force at first permanent molar (kg.).

TABLE VII.

DIMENSIONS OF THE MASTICATORY SYSTEM, LEVER ARM, LOAD ARM LENGTH AND MECHANICAL EFFICIENCY INDEX AND STATUS OF DENTAL DEVELOPMENT

ERUPTIVE STAGE	M	LEVER ARM	GI	GM1	GP	MEI I	MEI M1	MEI P
MONKEY #1								
DM2 OCCLUDING								
M1 ERUPTING								
M1 OCCLUDING	0	29.10	55.50	28.40	24.60	53.43	102.46	118.29
	7	30.00	61.40	31.70	28.00	48.86	94.63	107.14
M2 ERUPTING								
M2 OCCLUDING	19	39.00	75.20	44.10	35.20	51.86	88.43	110.79
M3 ERUPTING	27	41.10	82.00	47.20	37.60	50.13	87.71	109.31
M3 OCCLUDING	48	41.90	83.30	49.20	32.00	50.30	85.16	130.93
MONKEY #2								
DM2 OCCLUDING								
M1 ERUPTING								
M1 OCCLUDING								
M2 ERUPTING	0	29.20	60.50	31.00	22.60	48.26	94.19	129.20
M2 OCCLUDING	4	29.50	64.40	33.50	23.20	45.81	88.06	127.15
M3 ERUPTING	22	38.10	78.90	44.70	29.40	48.67	85.23	120.59
M3 OCCLUDING	28	41.80	81.50	46.40	31.00	51.29	90.08	134.83
	44	41.60	82.50	47.00	32.00	50.42	88.51	130.00
	51	41.60	83.60	48.00	32.00	49.76	86.66	130.00
MONKEY #3								
DM2 OCCLUDING								
M1 ERUPTING	0	23.10	49.70	21.60	18.80	46.43	106.94	122.87
M1 OCCLUDING	13	31.30	64.00	33.10	30.00	48.91	94.56	104.33
M2 ERUPTING								
M2 OCCLUDING	19	32.40	68.10	35.90	26.10	47.58	90.25	124.14
	27	34.10	74.60	40.30	30.10	45.57	84.62	113.29
M3 ERUPTING								
M3 OCCLUDING	45	36.18	76.50	44.10	28.80	47.18	82.22	125.48
	51	37.62	79.20	45.90	31.05	47.47	81.91	121.15

TABLE VII. (Cont'd)

DIMENSIONS OF THE MASTICATORY SYSTEM, LEVER ARM, LOAD ARM LENGTH AND MECHANICAL EFFICIENCY INDEX AND STATUS OF DENTAL DEVELOPMENT

ERUPTIVE STAGE	M	LEVER ARM	GI	GM1	GP	MEI I	MEI M1	MEI P
MONKEY #4								
DM2 OCCLUDING								
M1 ERUPTING								
M1 OCCLUDING	0	22.80	49.10	23.20	20.00	46.43	97.02	114.00
	13	30.30	59.20	30.30	27.30	51.18	100.00	110.98
M2 ERUPTING								
M2 OCCLUDING	19	34.50	67.00	36.00	27.00	51.49	95.83	95.83
	28	37.10	74.40	42.20	32.50	49.86	87.91	114.15
M3 ERUPTING	44	38.20	76.80	44.00	28.60	49.73	86.81	133.56
M3 OCCLUDING	51	40.00	81.00	45.80	29.00	49.38	87.33	137.93
MONKEY #5								
DM2 OCCLUDING	0	20.40	45.20	18.10	16.00	45.13	112.70	127.50
M1 ERUPTING								
M1 OCCLUDING	7	28.80	56.50	28.40	25.20	50.97	101.40	114.28
M2 ERUPTING	19	38.10	69.10	32.40	27.20	47.90	102.16	121.69
M2 OCCLUDING	28	38.60	78.00	41.90	31.10	49.48	92.12	124.11
M3 ERUPTING	48	38.50	85.00	48.20	30.00	45.29	79.87	128.30
M3 OCCLUDING								
MONKEY #6								
DM2 OCCLUDING	0	17.90	42.10	20.80	18.20	42.51	86.05	98.35
M1 OCCLUDING	14	26.70	55.10	26.20	23.00	48.45	101.90	116.08
	20	28.10	59.80	28.40	25.30	46.98	98.94	111.06
M2 ERUPTING	29	28.50	64.20	30.60	20.10	44.39	93.13	141.79
M2 OCCLUDING	44	29.88	66.60	35.10	24.48	44.86	84.90	122.45
M3 ERUPTING	52	29.80	68.40	29.15	29.70	43.56	76.12	100.33
M3 OCCLUDING								

TABLE VII. (Cont'd)

DIMENSIONS OF THE MASTICATORY SYSTEM, LEVER ARM, LOAD ARM LENGTH AND MECHANICAL EFFICIENCY INDEX AND STATUS OF DENTAL DEVELOPMENT

ERUPTIVE STAGE	M	LEVER ARM	GI	GM1	GP	MEI I	MEI M1	MEI P
MONKEY #7								
DM2 OCCLUDING	0	24.10	49.90	22.20	19.50	48.29	108.55	123.58
M1 ERUPTING								
M1 OCCLUDING		27.90	61.80	31.50	28.40	45.14	88.57	98.23
M2 ERUPTING	13	30.20	65.10	35.40	24.10	46.39	85.31	125.31
M2 OCCLUDING	19	33.10	70.80	39.50	29.30	46.75	83.79	112.96
	28	34.20	72.45	42.75	27.90	47.20	80.00	122.58
M3 OCCLUDING	51							
MONKEY #8								
DM2 OCCLUDING								
M1 ERUPTING								
M1 OCCLUDING	0	22.30	48.00	21.10	19.10	46.45	105.68	116.75
M2 ERUPTING								
M2 OCCLUDING	9	30.40	63.40	34.00	24.80	47.94	89.41	122.58
	15	34.10	69.20	37.50	27.60	49.27	90.93	123.55
	24	35.20	73.30	42.10	30.00	48.02	83.61	117.33
M3 ERUPTING	44	36.90	74.70	43.20	28.80	49.39	85.41	128.12
M3 OCCLUDING	47	36.90	76.50	43.65	30.60	48.23	84.53	120.59
MONKEY #9								
DM2 OCCLUDING								
M1 ERUPTING								
M1 OCCLUDING	0	31.70	64.10	35.90	26.00	49.45	88.30	121.92
M2 ERUPTING	13	36.10	72.00	42.20	31.80	50.13	85.54	113.52
M2 OCCLUDING	19	37.00	72.50	43.70	32.80	51.23	84.66	112.80
	41	37.90	73.80	44.60	34.00	51.35	84.97	111.47
M3 ERUPTING	50	39.00	74.10	44.00	33.90	52.70	88.63	115.04
M3 OCCLUDING								

TABLE VII. (Cont'd)

DIMENSIONS OF THE MASTICATORY SYSTEM, LEVER ARM, LOAD ARM LENGTH AND MECHANICAL EFFICIENCY INDEX AND STATUS OF DENTAL DEVELOPMENT

ERUPTIVE STAGE	M	LEVER ARM	GI	GM1	GP	MEI I	MEI M1	MEI P
MONKEY #10								
DM2 OCCLUDING								
M1 ERUPTING	0	27.10	52.00	24.90	22.00	52.11	108.83	123.18
M1 OCCLUDING	7	27.50	55.90	32.10	30.20	49.19	85.66	91.25
M2 ERUPTING	13	32.30	68.10	35.20	25.30	47.43	91.76	127.66
M2 OCCLUDING	22	36.40	77.20	42.00	30.80	47.15	86.66	118.18
M3 ERUPTING	35	40.59	81.00	47.00	31.32	50.11	86.38	129.71
M3 OCCLUDING	44	42.50	86.00	50.10	32.20	49.41	85.00	131.98
MONKEY #11								
DM2 OCCLUDING	0	26.20	52.10	23.10	20.00	50.29	113.42	131.00
M1 ERUPTING								
M1 OCCLUDING	13	31.10	65.00	31.80	28.20	47.84	97.79	110.28
	19	33.00	70.90	36.20	32.80	46.54	91.16	100.61
M2 OCCLUDING	28	37.30	78.20	40.10	33.00	47.69	93.01	113.03
M3 ERUPTING	48	37.20	86.10	45.60	29.00	43.20	81.15	128.27
	51	37.50	86.00	46.00	35.00	43.60	81.15	107.14
monkey #12								
DM2 OCCLUDING								
M1 ERUPTING								
M1 OCCLUDING	0	30.00	61.50	32.00	29.00	48.78	93.75	103.44
M2 ERUPTING	6	32.00	70.50	36.50	33.50	45.39	87.67	95.52
M2 OCCLUDING	19	39.80	82.50	45.10	34.60	48.24	88.24	115.02
M3 ERUPTING	28	41.30	84.10	46.20	37.00	49.10	89.39	111.62
M3 OCCLUDING	43	41.80	84.40	47.72	31.60	49.52	87.60	132.27
	51	42.68	87.78	49.47	32.98	48.62	86.27	129.41

TABLE VII. (Cont'd)

DIMENSIONS OF THE MASTICATORY SYSTEM, LEVER ARM, LOAD ARM LENGTH AND MECHANICAL EFFICIENCY INDEX AND STATUS OF DENTAL DEVELOPMENT

ERUPTIVE STAGE	M	LEVER ARM	GI	GM1	GP	MEI I	MEI M1	MEI P
MONKEY #13								
DM2 OCCLUDING	0	24.10	49.30	23.00	19.90	48.68	104.34	120.60
M1 ERUPTING								
M1 OCCLUDING	7	28.00	55.70	28.10	25.20	50.26	99.64	111.11
	13	28.10	57.90	29.20	26.30	48.35	95.89	106.46
	22	32.30	68.10	35.40	26.60	47.43	91.24	121.42
M2 OCCLUDING	35	34.70	74.80	41.80	30.80	46.39	83.01	112.66
M3 ERUPTING	42	35.40	75.70	42.40	31.50	46.76	83.44	112.30
M3 OCCLUDING								
MONKEY #15								
DM2 OCCLUDING	0	25.10	50.20	22.70	20.00	49.80	110.13	125.00
M1 ERUPTING								
M1 OCCLUDING	7	25.20	53.10	25.00	22.50	47.45	100.80	112.00
	13	28.40	60.50	29.70	26.40	46.94	95.62	107.57
M2 ERUPTING	22	31.10	66.20	33.60	24.00	46.82	92.26	129.16
M2 OCCLUDING	33	31.50	71.10	38.40	27.80	44.30	82.03	113.30
	39	35.40	75.20	41.80	31.04	47.07	84.68	114.19
M3 ERUPTING	45	35.00	78.00	42.50	32.00	44.87	82.35	109.37
MONKEY #16								
DM2 OCCLUDING	0	23.20	50.00	22.90	20.10	46.40	101.31	115.42
	7	27.10	54.80	28.10	23.70	49.20	96.42	113.92
M1 OCCLUDING	13	30.30	61.70	32.50	29.20	49.10	93.23	103.76
M2 ERUPTING	21	32.20	65.90	36.30	26.40	48.86	88.70	121.96
M2 OCCLUDING	33	32.30	71.80	39.40	29.60	44.98	81.97	109.12
M3 ERUPTING	44	33.40	76.90	43.70	27.50	43.43	76.43	121.01
M3 OCCLUDING								

TABLE VIII.

RELATIONSHIPS BETWEEN CROSS-SECTIONAL AREAS OF THE JAW ELEVATOR MUSCLES
AND THE MECHANICAL EFFICIENCY INDEX AT INCISOR AND MOLAR BITE POINT.

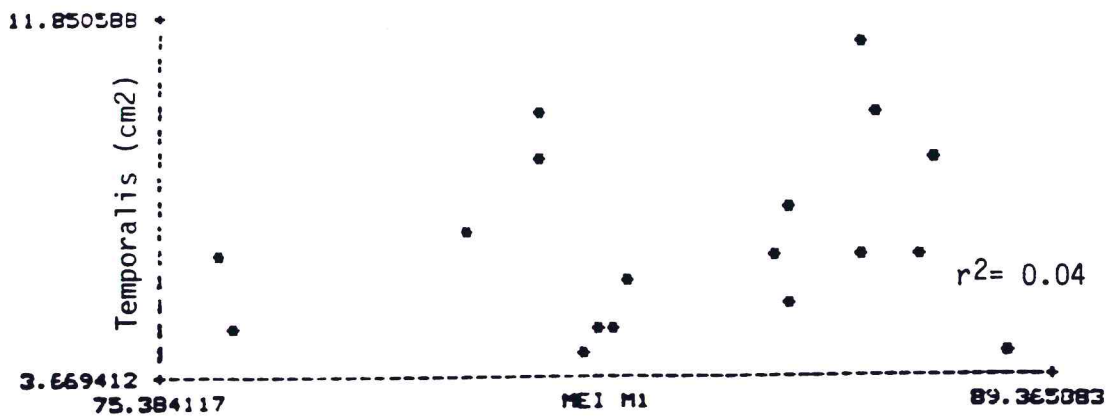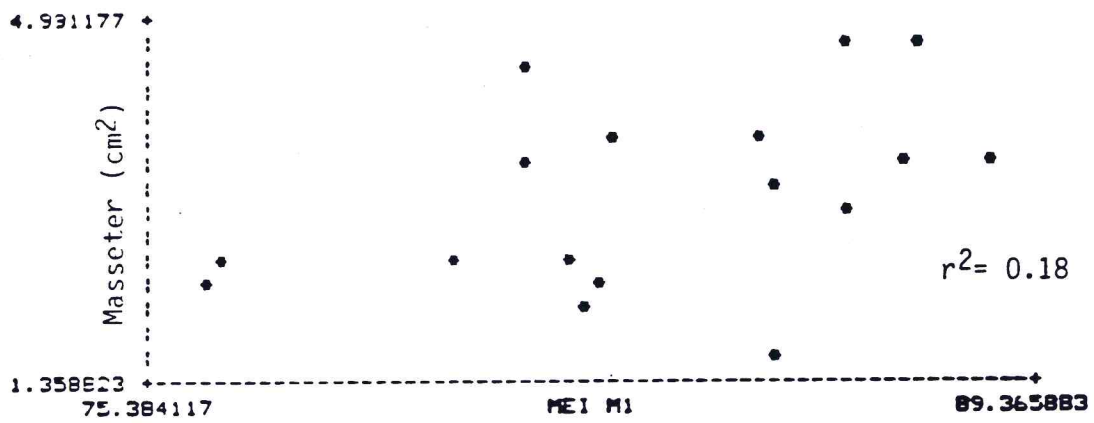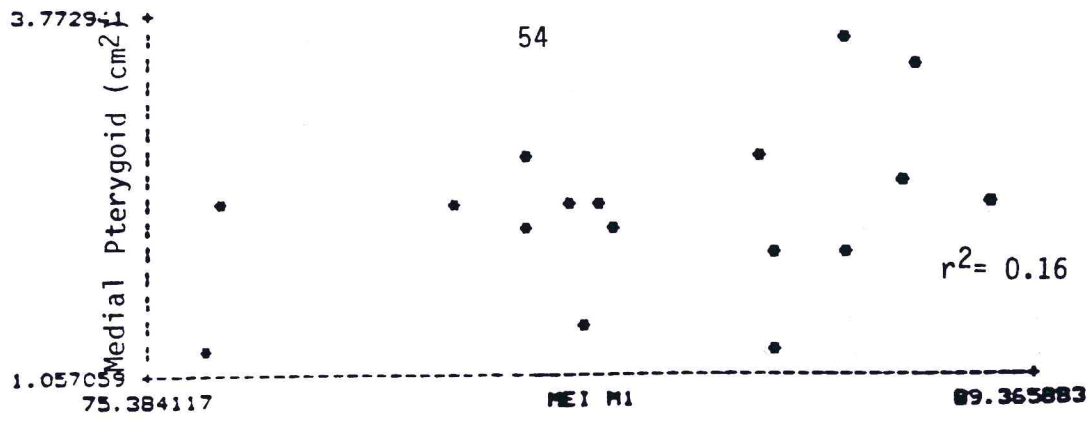| Cross-sectional Area and MEI at Incisor	M. Pterygoid	Masseter	Temporalis
Sample (n)	16.00	16.00	17.00
Correlation (r^2)	0.08	0.10	0.01
Slope	0.06	0.10	0.06
T-value	1.17	1.32	0.37
Total different			
Sample (n)	10.00	11.00	12.00
Correlation (r^2)	0.02	0.003	0.02
Slope	-0.01	0.03	-0.11
T-value	-0.37	0.18	-0.46
Cross-sectional Area and MEI at Molar			
Sample (n)	16.00	16.00	17.00
Correlation (r^2)	0.16	0.18	0.04
Slope	0.07	0.11	0.11
T-value	1.66	1.80	0.78
Total different			
Sample (n)	10.00	11.00	12.00
Correlation (r^2)	0.02	0.01	0.10
Slope	-0.39	0.26	-1.11

Figure 18. Scatter plots comparing cross-sectional areas of the jaw
elevator muscles (cm^2) and mechanical efficiency index at
first permanent molar bite point.

TABLE IX.

RELATIONSHIPS BETWEEN LEVER ARM AND LOAD ARM LENGTH AT INCISOR,
FIRST PERMANENT MOLAR AND POSTERIOR WEAR POINT OF THE TOOTH ROW.

Lever arm and Load Arm length (mm)	Incisor	M1	MP
Sample (n)	91.00	91.00	91.00
Correlation (r^2)	0.91	0.91	0.63
Slope	0.48	0.65	0.97
T-value	31.96*	30.68*	12.38*

TABLE X.

RELATIONSHIPS BETWEEN THE CROSS-SECTIONAL AREAS OF
TEMPORALIS AND MASSETER MUSCLES AND THE LEVER ARM.

Cross-sectional Area	Temporalis	Masseter
Sample (n)	27.00	25.00
Correlation	0.32	0.59
Slope	0.26	0.16
T-value	3.49*	5.85*

Figure 19. Scatter plots comparing the lever arm lengths (mm) and the load arm at incisor (a), first permanent molar (b) and posterior wear points of the tooth row (mm) (c).
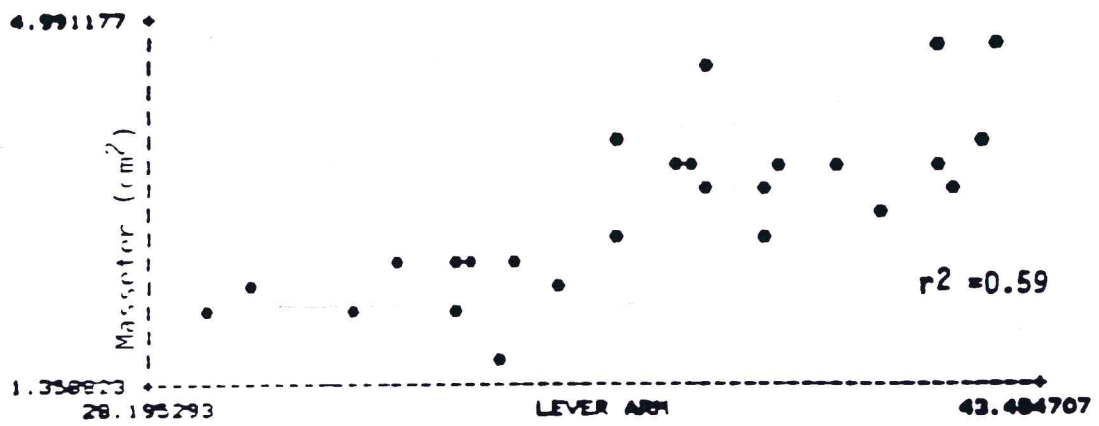
Figure 20. Scatter plots comparing lever arm lengths (mm) and the cross-sectional areas of the masseter muscle (cm^2).
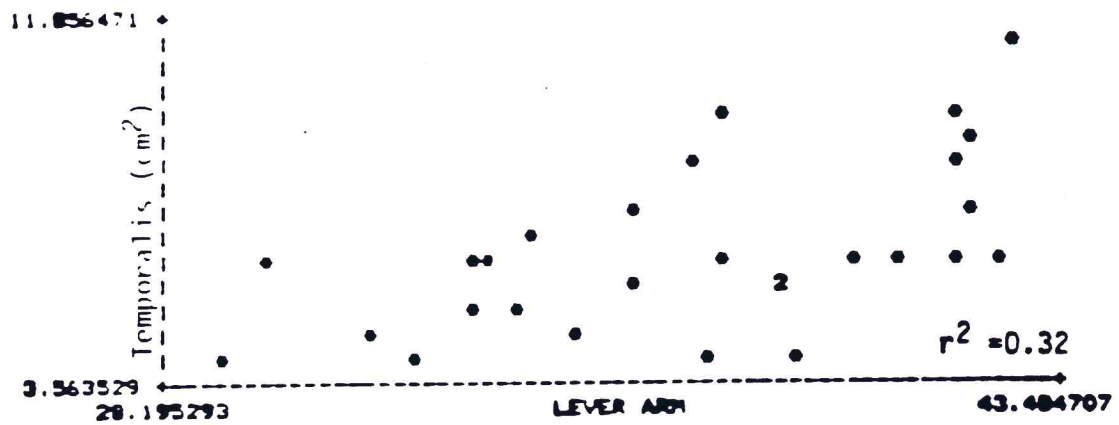

Figure 21. Scatter plots comparing lever arm lengths (mm) and the cross-sectional areas of the temporalis muscle (cm^2).

TABLE XI.

RELATIONSHIPS BETWEEN AGE AND THE MECHANICAL EFFICIENCY INDEX
AT INCISOR, FIRST PERMANENT MOLAR AND POSTERIOR WEAR POINT
OF THE TOOTH ROW.

MEI and Age (Mos.)	Incisor	M1	MP
Sample (n)	91.00	91.00	91.00
Correlation (r^2)	0.002	0.54	0.10
Slope	-0.005	-0.33	0.17
T-value	-0.43	-10.21*	3.23*

TABLE XII.

RELATIONSHIPS BETWEEN BODY WEIGHT AND MECHANICAL EFFICIENCY INDEX
AT INCISOR, FIRST PERMANENT MOLAR AND POSTERIOR WEAR POINT
OF THE TOOTH ROW.

Body Weight (kg) and MEI	Incisor	M1	MP
Sample (n)	77.00	77.00	77.00
Correlation (r^2)	0.0003	0.47	0.17
Slope	-0.28	-3.05	2.67
T-value	-0.17	-8.23*	4.01*

Figure 22. Graphic representation of age-related changes/differences in the mechanical efficiency index at the posterior wear point of the tooth row, first permanent molar and incisor bite point in monkey #3.
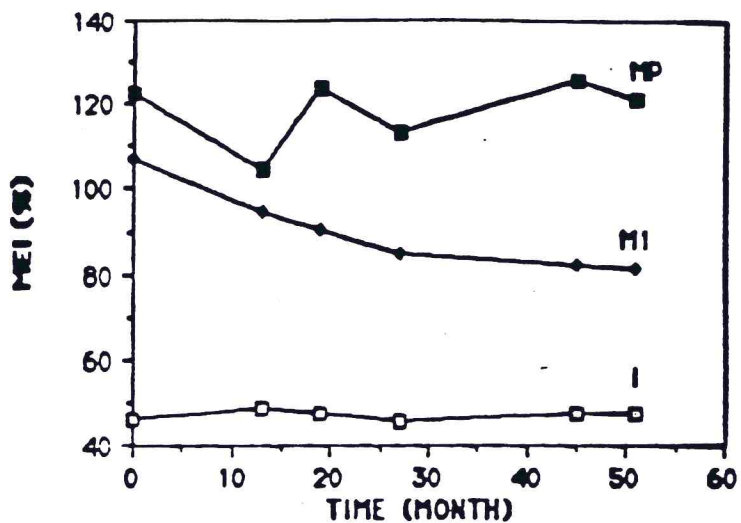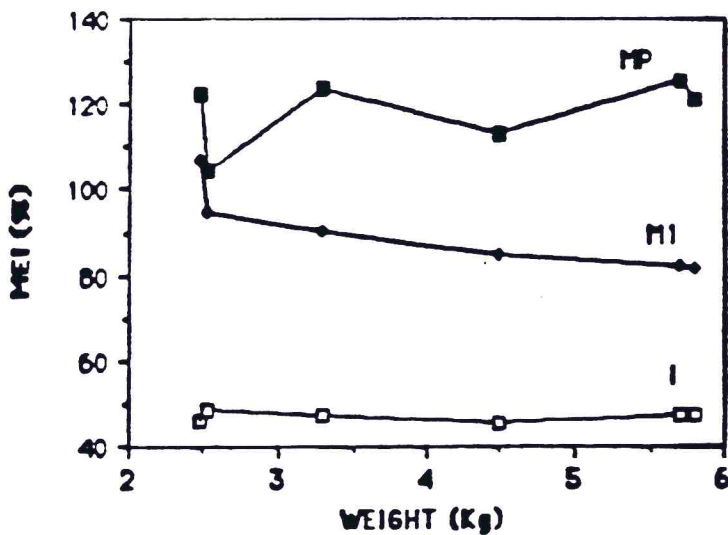

Figure 23. Graphic representation of weight-related changes/ differences in the mechanical efficiency index at the posterior wear point of the tooth row, first permanent molar and incisor in monkey #3.

TABLE XIII.

RELATIONSHIPS BETWEEN AGE AND MAXIMUM BITE FORCE CAPABILITIES
AT INCISOR, FIRST PERMANENT MOLAR AND SECOND PERMANENT MOLAR.

Bite Force (kg) and Age (mos.)	Incisor	M1	M2
Sample (n)			
Soft diet	27.00	35.00	23.00
Hard diet	52.00	59.00	41.00
TOTAL	80.00	95.00	65.00
Correlation (r^2)			
Soft diet	0.35	0.51	0.20
Hard diet	0.44	0.46	0.31
TOTAL	0.42	0.49	0.29
Slope			
Soft diet	0.22	0.48	0.41
Hard diet	0.29	0.51	0.53
TOTAL	0.28	0.50	0.50
T-value			
Soft diet	3.76*	5.99*	2.33*
Hard diet	6.35*	7.03*	4.22*
TOTAL	7.51*	9.36*	5.05*

TABLE XIV.

RELATIONSHIPS BETWEEN BODY WEIGHT AND MAXIMUM BITE FORCE
CAPABILITIES AT INCISOR, FIRST PERMANENT MOLAR
AND SECOND PERMANENT MOLAR.

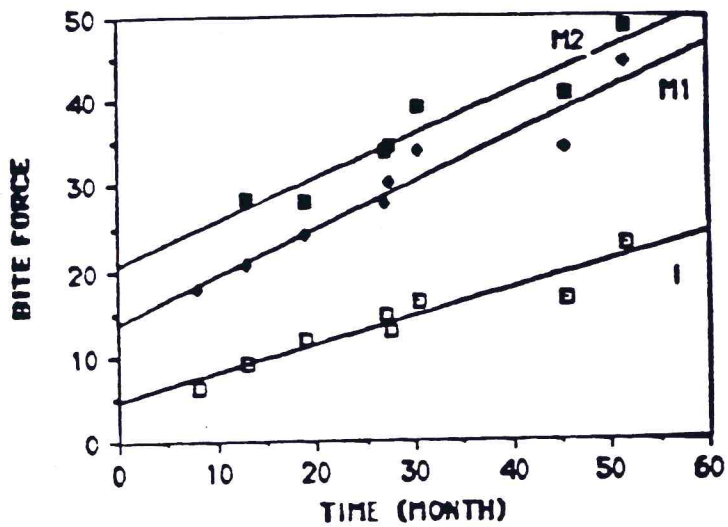| Bite Force (kg) and Body Weight (kg)	Incisor	M1	M2
Sample (n)			
Soft diet	27.00	35.00	53.00
Hard diet	51.00	58.00	41.00
TOTAL	79.00	94.00	65.00
Correlation (r^2)			
Soft diet	0.58	0.70	0.37
Hard diet	0.69	0.81	0.66
TOTAL	0.54	0.68	0.50
Slope			
Soft diet	2.57	5.30	6.34
Hard diet	4.23	11.14	9.03
TOTAL	3.41	6.46	7.58
T-value			
Soft diet	5.94*	8.86*	3.60*
Hard diet	10.64*	16.10*	8.89*
TOTAL	9.55*	14.06*	8.01*

Figure 24. A comparison of estimated age (mos.) and bite force capabilities (kg.) at second permanent molar, first permanent molar, and incisor of monkey 3.
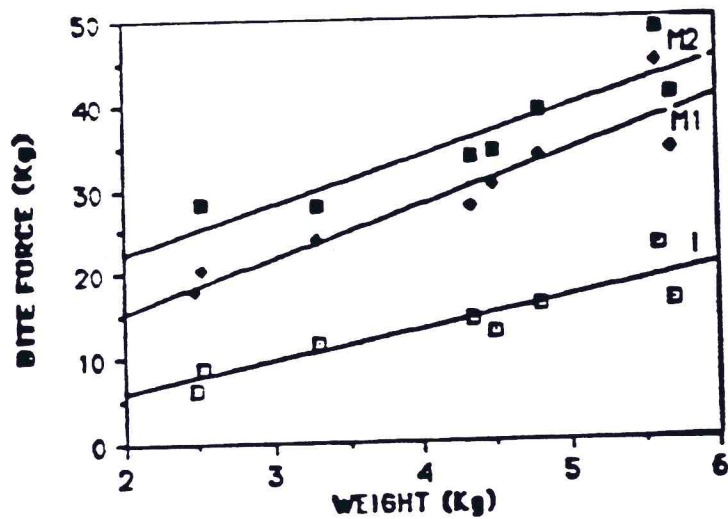

Figure 25. A comparison of body weight (kg.) and bite force capabilities (kg.) at second permanent molar, first permanent molar, and incisor of the monkey #3.

TABLE XV.
RELATIONSHIPS BETWEEN MAXIMUM BITE FORCE CAPABILITIES
AND MECHANICAL EFFICIENCY INDEX AT INCISOR
AND MOLAR BITE POINT.

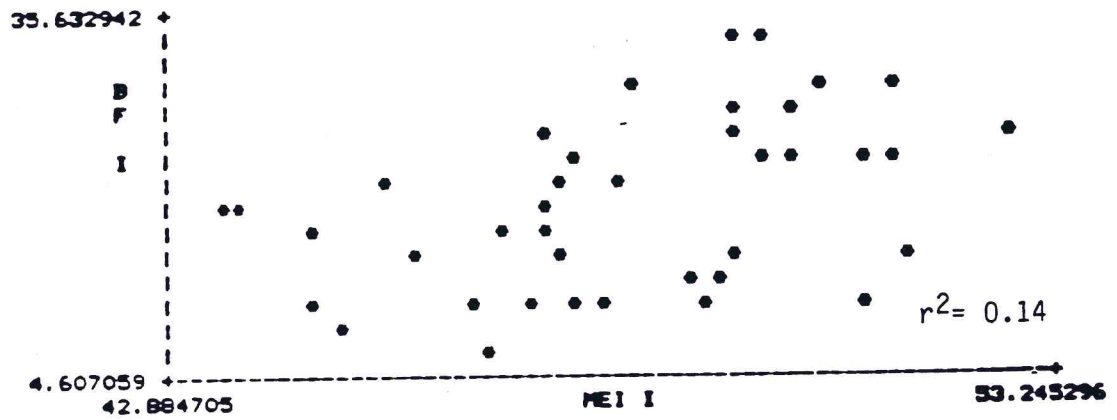| MEI (%) and Bite Force (kg)	Incisor	M1	M2
Sample (n)			
Soft diet	23.00	26.00	19.00
Hard diet	38.00	45.00	30.00
TOTAL	62.00	72.00	50.00
Correlation (r^2)			
Soft diet	0.03	0.42	0.08
Hard diet	0.18	0.27	0.05
TOTAL	0.14	0.30	0.07
Slope			
Soft diet	0.32	-1.07	0.29
Hard diet	1.32	-0.97	0.32
TOTAL	1.01	-1.00	0.33
T-value			
Soft diet	0.81	-4.22*	1.24
Hard diet	2.84	-4.04*	1.23
TOTAL	3.10*	-5.51*	1.88

Figure 26. Scatter plots comparing the mechanical efficiency index at incisor bite points and the bite force capabilities at incisor (kg.).
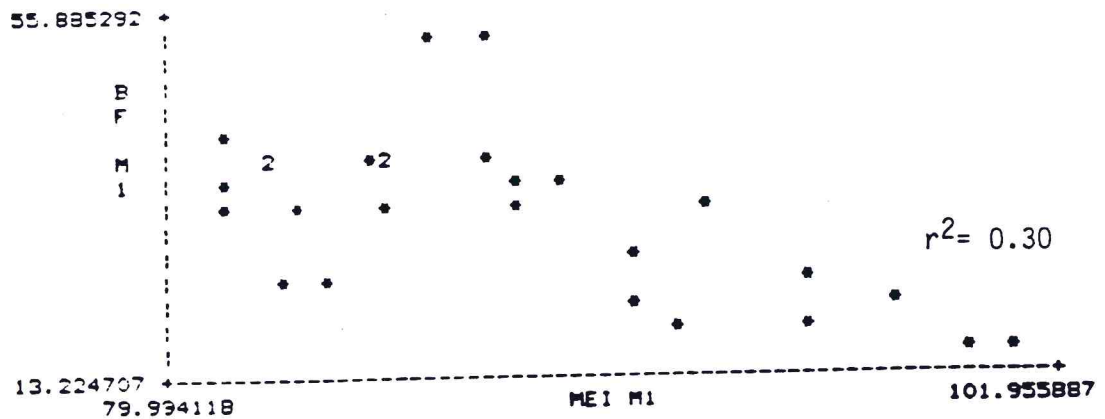

Figure 27. Scatter plots comparing the mechanical efficiency index at first permanent molar and the bite force capabilities at first permanent molar.
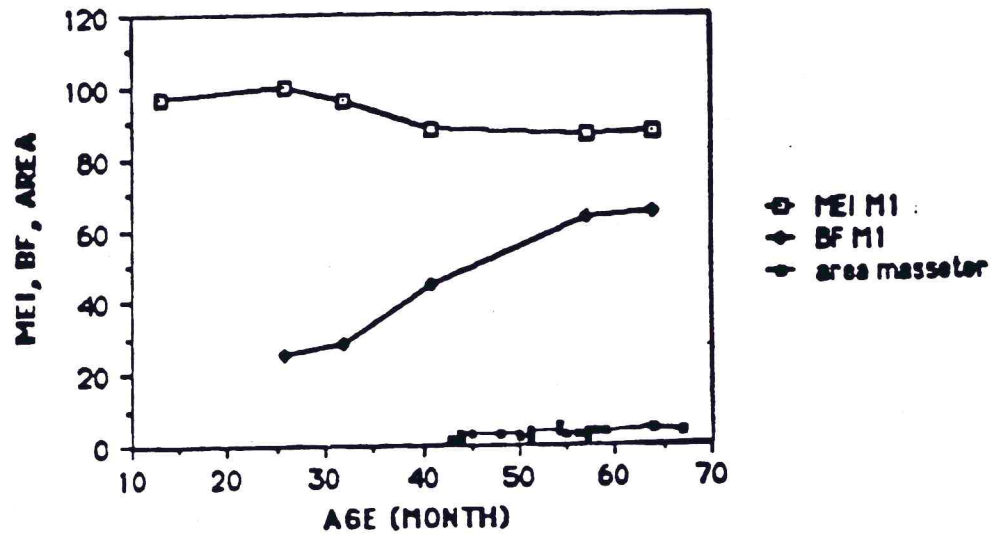
Figure 28. A comparison of chronological age (mos.) and the
mechanical efficiency index, the bite force (kg.), and
the cross-sectional areas of the masseter muscle (cm^2).

DISCUSSION

The present investigation is one of the first non-invasive attempts to characterize physiologic cross-sectional areas of masticatory muscles in live animals and is unique in its use of magnetic resonance imaging techniques to achieve that purpose. In this study the anatomy of the masticatory muscles in fifteen controlled-diet vervet monkeys is evaluated by a variety of means, with special attention given to magnetic resonance imaging.

Evaluation of the magnetic resonance methodology:

Magnetic resonance imaging was originally selected as a methodology in the hope that it would provide much better soft tissue contrast than other methods such as computed tomography or x-ray. Judging from figures provided in this report, e.g. Figures 8 and 9, it is clear that this technique does produce images with excellent detail and high resolution. The quality of the resolution allows clear separation of different soft tissues, an important capability insofar as this study is concerned. For example, during measurement of the masseter muscle, because of image detail it was easy to distinguish between the body of mandible, the musculature and the immediately overlying parotid gland. In contrast, efforts to obtain corroborative direct measurement of masseteric thickness through the use of a calibrated needle penetrating the skin and underlying tissues were confounded because there was no good way to account for the thickness of the skin, fascia and glandular tissues which overlie the masseter muscle. Because of the quality imagery and associated

66

analytic methods, this methodology also yields quantitative measurements which assess, with greater accuracy than previously possible, the cross-sectional area of the jaw elevator muscles in the living animals.

Additionally, whereas in the past measurements of some components used in biomechanical analyses were taken directly from dry skulls, e.g. the zygomatic fossa area (see Oyen, 1982, for example), magnetic resonance imaging makes it possible to actually evaluate all anatomical structures in vivo, including those which occupy the zygomatic fossa (see p. 76).

With regard to characterization of the jaw elevator muscles, scanning plane and angulation selections are somewhat subject to error since they rely upon subjective visual estimation of the long axis of the muscles in question. However, in this study inaccuracies in scanning plane and angulation had little effect on the cross-sectional area measurements. Only minor differences in muscular cross-sectional areas were detectable within a range of ten degrees. For example, using an angle which differed by five degrees, we found the cross-sectional area of the medial pterygoid muscle changes only 5.71%. Moreover, Weijs and Hillen (1984), working with computed tomography scans and human materials, concluded that slight variations involving scanning plane position and angulation are not critical, as the muscle cross-section tends to remain stable over a fairly wide of position and angles.

As demonstrated in this report, the advanced post-processing capabilities of magnetic resonance imaging provide data displays and

facilitate analytic functions which are very useful for quantitative research. For example, instant oblique reconstruction is a display function that makes it possible to manipulate an image plane in any direction in order to obtain a desired view of a given structure, such as the cross-section perpendicular to the long axis of a masticatory muscle. Another analytic function, the track cursor, allows measurement of cross-sectional areas of masticatory muscles directly from the magnetic resonance images using the trackball to outline the enclosed area. Such methodological capabilities made it relatively easy to obtain quite accurate measurements of the jaw elevator muscle through use of non-invasive, non-radioactive techniques. Thus, based on its applications in this study, magnetic resonance imaging may be an ideal diagnostic technique for such purposes. Computed tomography, because of its poor resolution in soft tissue images and radiation concerns, cannot compare in usefulness.

Magnetic resonance imaging did prove to have some limitations and disadvantages. One limitation associated with this technique involves possible loss of precision through a compromise involving slice thickness. In this study, the slice thickness of each adjacent section was 3.5mm (for a definition of "slice thickness", see Appendix Section). As the magnetic resonance system was designed for human proportions and signal intensities, 3.5mm is considered a "very thin slice" relative to human anatomical structures. In vervet monkeys, which are much smaller, a 3.5mm slice is much larger. As indicated earlier, this thickness was chosen over thinner sections in

order to incorporate a greater number of protons into the field, which increases the signal strength that determines the quality of the image. While a reduction in slice thickness would offer insurance against missing the largest muscle cross-sectional area between two slices, it would involve a sacrifice of signal strength at the same time, and the resulting image would have less visible detail. The anatomical structure of each elevator muscle is relatively small and relatively low in proton density. Moreover, since the muscles are in the anisotropic mode (one of the two pixel dimensions is unequal to the others) this mode will effect instant oblique reconstruction by degrading the resolution. Consequently, to obtain an adequate signal intensity in either the coronal or transverse sections under such conditions is was necessary to resort to relatively thick sections in these small animals to achieve optimum contrast resolution. In a very small structure, if inadequate coronal or transverse sections are obtained, efforts at instant oblique reconstruction will be compromised. In a study of larger animals such as humans, the resolution will be improved, but it will depend on which structure is of interest. Regions of high proton density will produce the strongest signals, and, since water and lipids are the most effective protons, regions of high water content such as the brain or glands are known to produce very effective images.

A second limitation of magnetic resonance imaging is related to the method used for cross-sectional area determinations. The cursor used to draw the circumference of the cross-sectional area of

the chosen muscle group was highly sensitive to any slight movement and also was affected by the pixel size (computer term for a picture of the smallest discrete part of the digital image display). This frustrated attempts to obtain a very smooth curve. However, this variance is probably not much greater than the actual limitations of the pixel size which for this study is 0.78mm on a side. The dimensions of the voxel element is 0.78mm x 0.78mm x 3.5mm are the theoretical limitations of measurement. This displacement might exaggerate or underestimate the actual measurements. Careful manipulation, multiple measurements and cautious interpretation are the only recourse in this situation.

A final consideration of problems related to the chosen study technique must acknowledge that blood vessels, nerve fibers and fascia were very difficult to distinguish from the muscle fibers in the scan since they occupied a relatively small proportion of the slice thickness. The inability of magnetic resonance imaging to distinguish and accommodate for these components under the condition for this study may have affected the value of the measurements. This is of particular consequence with regard to the temporalis muscle and the zygomatic fossa, a physical feature that was not directly assessed in this study. In order to distinguish these structures, it was, at times, necessary to increase contrast by change to T1 or T2 and by using a different pulse sequence (see Appendix). This alteration unfortunately, always results in increased scanning time. Already the procedure required the anesthetized monkey to lie still for a long period of time (approximately twenty minutes).

Prolongation of the scan time increases the likelihood of movement, and any motion during the scan interval results in a blurring of the images.

These problems, largely unavoidable during the course of this initial study, will be resolved by more sophisticated technology. Already steps are underway to obtain a precise evaluation of the zygomatic fossa and its contents. Additionally, Picker International is currently in the process of developing a three-dimensional data acquisition procedure for magnetic resonance imaging which will considerably enhance resolving power over the two-dimensional technique. The new, three-dimensional imagery will increase overall spatial resolution with instant oblique reconstruction. Three dimensional imaging will also eliminate the need for both coronal and transverse scans and give better signal-to-noise ratio for equal resolution.

Evaluation of data from magnetic resonance and other data:

Results of analysis of the magnetic resonance data are consistent with findings of Weijs and Hillen (1985) who used computed tomography to study the cross-sectional areas of human jaw muscles in cadavers. In their analysis, Weijs and Hillen determined that the masseter and medial pterygoid cross-section areas had the highest positive correlation and that the temporalis and medial pterygoid cross-sectional areas had the lowest. These investigators reasoned from the functional point of view that the masseter and medial pterygoid muscles shared the angular process as an insertion area and each compensated the other's transverse force component, applied to

the angle of the mandible. From the human study, it could be argued that the high correlation found between the cross-sectional areas of these masseter and medial pterygoid muscles was due to their similar morphology and that the low temporalis-medial pterygoid correlation somehow is a function of the problematic fan shape of the temporalis muscle. Based on this interpretation, the agreement between these results obtained from human and monkey studies concerning muscular correlations is consistent with our initial assumption that the vervet monkey would prove to be a good animal model of human craniofacial biomechanics.

The correlation between the cross-sectional areas of the masseter, medial pterygoid and temporalis muscles and body weight was highly significant, (r^2 = 0.58, 0.62 and 0.51 respectively). A larger animal, with greater body weight, tends to have larger muscles of mastication. There were some exceptions involving animals of lesser body weight who had large muscles. This may be attributed to the functional demand of mastication, with a more challenging diet resulting in increased bite force capabilities.

No significant correlation was found to exist between chronological age and the cross-section area of the muscles (Figure 16). Several factors should be noted in interpreting these chronological age-related results. First, at the onset of the experiments, in almost all the monkeys the third permanent molars were erupting or were functionally occluding, indicating that the animals were reaching dental maturity. It is likely that if these animals had been studied with magnetic resonance imaging beginning in

infancy or shortly after entering puberty, more significant relationships between cross-sectional area of the muscles and ages might have emerged. As it was, each animal was studied as a part of a larger group of essentially dentally mature animals which exhibited variations in size, body weight and chronological age. Some were older, but had smaller bodies and smaller muscle sizes; others were younger, but had larger bodies and larger muscle sizes. For example, animal #9 was 80 months old, his body weight was 5.4 kg, and animal #10 was 59 months old, with a body weight of 6.1 kg. Given such variations, the low correlation between chronological age and the cross-sectional areas of the muscles is not unexpected. As already indicated in the Results Section, some indication of actual growth related changes between the initial and final magnetic resonance imaging data collection times were provided by the five youngest monkeys in our sample. These data give some idea about how much change occurs in the last phase of dental maturation. These changes, although somewhat limited, support the notion that during active growth there would be a much higher correlation between chronological age and muscle cross-sectional area.

The maximum bite force capabilities were assessed by the bioelectrical stimulator and the bite force transducer (see Methods Section). The elicited bite forces were recorded at the maximum strength that a monkey could generate, so non-elicited bite force was not assessed. Moreover, according to the protocol used in this study, during each bite force test stimulation all the elevator muscles were stimulated, irrespective of the bite point, e.g. incisor

or molar loading. It follows that test outputs so elicited <u>must</u> differ from the normal, non-test functions since, during normal biting or chewing behavior, individual jaw elevator muscles are differentially recruited. For example, according to Walker (1978), during incision, the strong activity occurs in the medial pterygoid muscle, whereas activity in the temporalis muscle is reduced by at least half. During mastication (posterior loading), the elevating superficial fibers of the masseter muscle are very active. The medial pterygoid is the first of the elevators to act in the chewing cycle, while the temporalis muscles are active in free lateral movement. Swenson (1964) states that the temporalis does not participate in biting, especially in anterior biting. Moller (1966) agreed with MacDougall and Andrews (1955) and Greenfield and Wyke (1956) that the temporalis is relatively inactive during incisor biting, while masseter was moderately active. In addition, Moller (1966) found that the medial pterygoid was highly active during incisal biting. In contrast, the protocol used in the current study does not allow for differential evaluation of jaw muscle activities. It must be borne in mind that this bite force protocol was determined as a method to assess effects of total tetanic contractions. In this method it was assumed that the relationship between the normal bite force and the maximum bite force had high correlation, since the bite force capabilities were generated by the same musculoskeletal components.

The relationship between force magnitude and geometry of the masticatory muscle is of critical importance. Based upon his study

of the human knee, Knuttgen (1976) established that the maximum force which can be produced by a muscle is directly proportional to its cross-sectional area. The present study shows (Figure 17) a positive relationship between the cross-sectional areas of the masseter and medial pterygoid muscles and the maximum bite force capability ($r^2 = 0.24$, 0.35 respectively). However, a lower correlation was found between the temporalis muscle and bite force at the incisors ($r^2 = 0.093$), and a low correlation was found at the molars ($r^2 = 0.17$). Once again these correlations probably are a reflection of the anatomical functional demand made upon each muscle, since the masseter and medial pterygoid muscles have a broader insertion, a shorter line of action and are relatively closer to the dentition than the temporalis muscle. Present results show that the masseter and the medial pterygoid has the highest positive correlation to the bite force capabilities. It is likely that the masseter-medial pterygoid complex generated forces greater than the temporalis muscle because the physiological cross-sectional area of masseter and medial pterygoid (in humans) made up about 57% of the total cross-sectional area for the jaw elevator muscles (Schumacher, 1961). Hylander (1975) also concluded that the masseter and medial pterygoid complex provided the primary substantial muscle forces and that the anterior part of the temporalis muscle made only a lesser contribution. Despite numerous electromyographic studies, little can be added in further analysis of temporalis activities, there being considerable unresolved disagreement between workers (Warwick et al, 1973).

Some of these experimental results seem to conflict with the hypothesis that masticatory muscle force is meaningfully correlated with cross-sectional area of the zygomatic fossa (Oyen, et al., 1979; Oyen, 1982; Russell, 1983; Rangel, 1985). These investigators, using dry skulls, estimated the bite force potential by using the area of the zygomatic fossa to provide some indication about the cross-sectional area of the temporalis muscle. Using magnetic resonance imaging of the transverse section of the temporal fossa, the present study found not only the temporalis muscle, but some fibers from the masseter muscle, lateral pterygoid muscle, coronoid process and some adipose tissue represented in that area. It remains to be determined exactly what role these structures play in influencing the size of the zygomatic fossa. It seems clear, however, the estimated cross-sectional area of the reconstructed zygomatic fossa is misleading. It is equally clear from in-vivo studies using advanced technology like the current study that it is necessary to re-evaluate earlier interpretations of bite force potential as measured in relation to the zygomatic fossa. In particular, consideration should be given to the high correlations that have been reported between lever arm length and zygomatic fossa area (r^2 = 0.86, p < .00001) in olive baboons (Oyen, et al., 1979). In subsequent analyses, serious consideration should be given to the use of measures which allow greater differentiation, e.g. magnetic resonance imaging, computer tomography and/or actual dissections.

From our experiments, we confirm that the mechanical efficiency index values at the incisor bite point are less than 100%

and the index values at the posterior tooth bite point exceed 100% (TABLE VII.). As the mechanical efficiency index increases, it becomes easier for the involved muscle to produce a greater bite force (Oyen, 1979, 1982; Rangel, 1984).

Regressions comparing the lever arm and load arm lengths showed that these parameters are highly significantly correlated (r^2 = 0.91). This correlation may be understood on the basis on an explanation by Enlow (1966), who postulated that the entire naso-maxillary complex is displaced anteriorly by displacement or translation by growth at the maxillo-facial sutures in conjunction with the deposition of bone in the area of the maxillary tuberosity. This displacement of the maxilla enables the lever arm and the load arm to enlarge simultaneously. This would result in a lengthening of the lever arm and maintenance of mechanical efficiency, an increase in the area of attachment for the masseter muscle, and it would also contribute to an increase in the zygomatic fossa area.

It is clear from the results of the present study that the lever arm shows strong correlation with the cross-sectional area of the masseter muscle. This makes sense since the most anterior point of origin of the masseter muscle is zygomaxillare, by convention the landmark on the upper jaw used to define the lever arm. Accordingly, it was not unexpected that these two features would have high correlation with each other. However, the lever arm and the cross-sectional area of the temporalis muscle showed a lower correlation. This may be explained by the complicated, fan shaped morphology of the temporalis muscle. It is perhaps not possible to

obtain an exact cross-sectional area of the temporalis muscle. The anterior fiber must be sectioned perpendicular to its long axis, whereas the posterior fiber is sectioned obliquely.

The cross-sectional area of the temporalis muscle and the mechanical efficiency index at the molar bite points showed no correlation (TABLE VIII). However, a low but statistically significant correlation was found between the cross-sectional area of the masseter and medial pterygoid and the mechanical efficiency index. These outcomes were unexpected because it was felt that, in a given monkey, the cross-sectional area of the muscle and its mechanical efficiency index should be highly related. Failure to find a strong correlation may be explained by several factors. First, inter-individual rather than longitudinal data were used in these analyses. Some monkeys had the same mechanical efficiency index, but most differed in the size of their cross-sectional area of muscle and in their bite force capabilities. Such a population-based approach is subject to more statistical variation and error, including variations in age, body weight, dietary consistency, and neuromuscular and genetic make-up and can obscure trends that might be better observed in longitudinal analyses.

The mechanical efficiency index at the incisor region remains relatively constant during growth and therefore shows no correlation to age. The most likely explanation for this is that the anterior displacement of the midface (the lever arm) keeps pace with anterior displacement of the incisors (the incisal load arm), resulting in a

relatively uniform anterior displacement of the entire facial complex.

The mechanical efficiency index at the molars always is higher than at the incisors, and shows an inverse correlation with age (Figure 22). The rationale for this is that the first molar undergoes a mesial drift which exceeds the constant relationship of the lever arm at the zygomatic process. During growth, as the first molars drift mesially, the load arm lengthens and the mechanical efficiency index decreases.

The mechanical efficiency index at posterior teeth showed an oscillating pattern and tended to increase with growth. The oscillating pattern seems to be related to the eruption of the permanent molars into occlusion, which initially increases the mechanical efficiency index, only to have it decrease again following the mesial drift of that molar. The overall mechanical efficiency index at posterior bite point increased with the eruption of the third molars. In a recent analysis, Oyen and Teaford (1988) found that the interval between the time of eruption and the onset of attrition took only eight weeks. These investigators have tentatively concluded that the dynamic process of tooth eruption and attainment of functional occlusion occurs very rapidly. If they are correct, in growing vervet monkeys, the mechanical efficiency index increases rapidly, then drops slowly during the non-eruptive stages.

The animal's bite force capabilities increased with age, but never exhibited a correlation as high as the correlation between bite force capabilities and body weight. This is most likely explained by

the differences in masticatory function between the animals, since the bite force capabilities are related to the cross-sectional area of the jaw elevator muscles. Some animals are old but have small bodies and muscles, some are young but have large bodies and muscles. Both correlation values (between bite force capabilities versus age or versus body weight) were higher in the hard diet group. In the soft diet group, the elevator muscles did not encounter the same functional demands as those monkeys fed with the hard diet. There is an increasing awareness that changes in muscle fiber distribution and size must be considered the result of neuromuscular alterations related to a different biting and chewing pattern. Kiliaridis et al. (1985) found that changes in the consistency of diet altered masticatory function in rats, and that the alteration in the masticatory function, in turn, caused changes in the composition and size of the masticatory fibers.

SUMMARY AND CONCLUSIONS

In this experimental primate study, magnetic resonance imaging and a variety of other methods, including in vivo bite force measurement and standard radiographic cephalometry, were used to investigate and further our understanding of masticatory biomechanics. The application of magnetic resonance imaging, using the Instant Oblique Reconstruction data display option, demonstrated a methodology capable of achieving high accuracy and excellent detail in this study of the cross-sectional area of the jaw elevator muscles. The easily replicable data display and analytic functions proved valuable in this quantitative research. Apart from an inability to sufficiently reduce the thickness of slice sections due to conditions that were somewhat exaggerated in this specific study, magnetic resonance imaging shows promise as an ideal technique for quantitative, non-invasive evaluations of soft-tissues and structures.

Based on statistical analyses, which included correlation analysis, the Student's t-test, and analysis of variance, the following results were obtained: Significant correlations ($p < .05$) were found between parameters of the masticatory system including maximum elicited in vivo bite force and cross-sectional areas of the masseter muscle at the level of $r^2 = 0.35$, the medial pterygoid at the level of $r^2 = 0.24$, and the temporalis at the level of $r^2 = 0.17$; masticatory lever arm lengths with masticatory load arm lengths at

81

the level of r^2 = 0.91. Masticatory lever arm lengths correlated with the cross-sectional areas of the masseter muscle at r^2 = 0.59, with the temporalis muscle at 0.32. Correlations of 0.44 and 0.69 were observed between maximum bite force and chronological age and bite force and body weight in monkeys raised on a "hard" diet. In monkeys raised on a "soft" diet, these correlations were reduced to 0.35 and 0.58 respectively.

Based on these results, several interpretations were offered. Similarity in correlations between the cross-sectional areas of the jaw elevator muscles reported here in monkeys and earlier in humans confirm the assumption that the vervet monkey is a good animal model of human craniofacial biomechanics. The correlations between bite force and cross-sectional areas are indicative of a functional integration of these two features. The low correlation between the temporalis cross-section and bite force may be seen as a reflection of the complex structure of that muscle. This observation may be related to the apparent conflict between the working hypothesis which links zygomatic cross-sectional area and temporalis size with bite force. It is clear that this hypothesis needs reevaluation. The difference observed in correlations associated with bite force between monkeys fed hard and soft diets can be taken as an indication that dietary manipulation has resulted in, or contributed to, the range of variation in bite force capability observed in the soft diet monkeys. Caution must be used in interpreting this aspect, however, because of inherent variability in this small sample.

Magnetic resonance imaging and allied methods show potential for application in areas of clinical research such as orthodontics and craniofacial surgery. No previous studies have been capable of recording measurable alterations in muscular morphology with the same accuracy as studies that measured alterations in skeletal morphology. Because of such advantages, this methodology should be useful in clarifying pre- and post-treatment changes in orthodontics practice or orthognatic surgery.

Finally, this investigation provides baseline information which should have application in further studies of biomechanics, muscular physiology, craniofacial biology and anthropology aimed at characterizing normal growth and developmental processes.

BIBLIOGRAPHY

Ahlgren, J. and Owall, B. (1970) Muscular activity and chewing force: A polygraphic study of human mandibular movements. Archives of Oral Biology, 15: 271.

Andreson, V. and Haupl, K. (1936) Funktions-Kieferorthopadie. Berlin: Herman Meusser.

Anthony, R. (1903) Introduction a' l' etude experimentale de la morphogenie. Bull. et Mem. Soc. d' Anthrop., Paris, V(4): 199-145.

Aronson, S.A., Holst, L. and Selvik, G. (1974) An instrument for insertion of radiopaque bone markers. Radiology 113: 733.

Avis, V. (1961) The significance of the angle of the mandible: An experimental and comparative study. Am. J. Phys. Anthropol., 19: 55-61.

Barber, C.G., Green, L.J. and Cox, G.J. (1963) Effects of the physical consistency of diet on the condylar growth of the rat mandible. J. Dent. Res. 42: 848-851

Beecher, R.M. and Corruccini, R.S. (1981) Effects of dietary consistency on craniofacial and occlusal development in the rat. Angle Orthod. 51: 61-69.

Bjork, A. (1968) The use of metallic implants in the study of facial growth in children: Method and application. Am. J. Phys. Anthropol. 29: 243-354.

Blakesley, D. (1985) Magnetic resonance imaging basic principles for operators. Picker International continuing education program.

Bouvier, M. and Hylander, W.L. (1981) Effect of bone strain on cortical bone structure in macaques (Macaca mulatta). J. Morpho. 167: 1-12.

Boyd, T.G., Castelli, W.A. and Huelke, D.F. (1967) Removal of the temporalis muscle from its origin: Effects on the size and shape of the coronoid process. J. Dent. Res. 46: 997-1001.

Brawley, R.E. and Sedwick, H.J. (1940) Studies concerning the oral cavity and saliva. Biting pressure and measurements of biting pressure in children. Am. J. Orthod. and Oral Surg. 26: 41-46.

Carlson, D.S. (1985) Craniofacial biology as "normal science." In New vistas in orthodontics, Johnson, L.E. (ed.) Philadelphia: Lea and Febiger, Chapter 2, pp. 12-37.

Cavalancia, J.A. (1985) The Relationship of Forceful Chewing and Palatal Form in the Vervet Monkey (Cercopithecus aethiops). Master's Thesis, Case Western Reserve University School of Dentistry, Cleveland, Ohio.

Damadian, R. (1971) Tumor detection by nuclear magnetic resonance. Science 171: 1151-1153.

Damadian, R., Goldsmith, M. and Minkoff, L. (1977) NMR in cancer: XVI Fonar image of the live human body. Physiological Chemistry and Physics 9: 97-100.

Dechow, P. and Carlson, D.S. (1983) A method of bite force measurement in primates. J. Biomech. 16: 797-802.

Endo, B. (1966) Experimental studies on the mechanical significance of the form of the human facial skeleton. J. Fac. Sci. Univ. Tokyo, Sect. V (Anthrop.) 3: 1-186.

Enlow, D.H. (1983) Handbook of Facial Growth, 2nd ed. Philadelphia: W.B. Saunders Company.

Enlow, D.H., Harvold, E.P., Latham, R.A., Moffett, B.C., Christiansen, R.L. and Hausch, H.G. (1977) Research on control of craniofacial morphogenesis: An NIDR state-of-the-art workshop. Am. J. Orthod. 71: 509-530.

Enlow, D.H., Moyers, R.E., Hunter, W.S. and McNamara, J.A. (1969) A procedure for the analysis of intrinsic facial form and growth. Am. J. Orthod. 56: 6-23.

Frankel, R. (1980) "A functional approach to orofacial orthopedics." Br. J. Orthod. 7: 41-51.

Genberg, R.W. (ed.) (1987) Image characteristics of field echo pulse sequences. In News, Views and Reviews for VISTA MR Users. Vol. 2, No. 4, pp. 20-22.

Greenfield, B.E. and B.D. Wyke (1956) Electromyographic studies of some of the muscles of mastication. Brit. Dent. J. 100: 129-143.

Horowitz, S.I. and Shapiro, H.H. (1951) Modification of mandibular architecture following removal of temporalis muscle in the rat. J. Dent. Res 30: 276-280.

Horowitz, S.1. and Shapiro, H.H. (1955) Modification of skull and jaw architecture following removal of the masseter muscle in rat. Am. J. Phys. Anthropol. 13: 301-308.

Hylander, W.L. (1975) The human mandible: Lever or link? Am. J. Phys. Anthropol. 43: 227-242.

Hylander, W.L. (1979) Mandibular function in Gagalgo crassicadatus and Macaca fascicularis: An in vivo approach to stress analysis of the mandible. J. Morphol. 159(2): 253-296.

Ingervall, B. and Helkimo, E. (1978) Masticatory muscle force and facial morphology in man. Arch Oral Biol. 23: 203-206.

Jenkins, G.N. (1966) The Physiology of the Mouth. Oxford: Blackwell Scientific Publications, pp.422-426.

Johnston, L.E. (1976) "Functional matrix hypothesis: Reflections in a jaundiced eye." In: Factors Affecting the Growth of the Midface, McNamara, J.W.J. (ed.). Craniofacial Growth Series, Ann Arbor Center for Human Growth and Development, University of Michigan, pp. 131-169.

Kiliaridis, S., Engstrom, C., and Thilander, B. (1985) The relationship between masticatory function and craniofacial morphology. Eur. J. Orthod. 8(4): 271-279.

Lauterbur, P.C. (1973) Image formation by induced local interactions examples of employing NMR. Nature 1973 242: 190-191.

Linderholm, H. and Wennstrom, A. (1970) Isometric bite force and its relation to general muscle force and body build. Acta Odont. Scand. 28: 679-689.

Mansour, R.M.and Reynik, R.J. (1975) In vivo occlusal forces and moments: I forces measured in terminal hinge position and associated moments. J. Dent. Res. 54: 114-120.

MacDougall, J. D. B. and Andrew, B.L. (1983) An electromyographic study of the temporalis and masseter muscles. J. Anat. 87: 37-45.

Mansfield, P., Maudsley, A.A. and Baines, T. (1976) Fast scan proton density imaging by NMR. J. Physics E 9: 21-278.

Mcfee, C.E. and Kronman, J.H. (1969) Cephalometric study of craniofacial development in rabbits with impaired masticatory function. J. Dent. Res. 48: 1268.

McNamara, J.A., Jr. (1972) Neuromuscular and skeletal adaptations to altered orofacial function. Monograph 1. Ann Arbor, Michigan, Center for Human Growth and Development, University of Michigan, 1972.

McNamara, J.A., Jr. (1973) Neuromuscular and skeletal adaptations to altered function in the orofacial region. Am. J. Orthod. 64:578-606.

McNamara, J.A., Jr. (1984) Dentofacial adaptations in adult patients following functional regulator therapy. Am. J. Orthod. 85: 57-71.

McNamara, J.A., Jr. and Carlson, D.S. (1979) Quantitative analysis of temporomandibular joint adaptations. Am. J. Orthod. 76: 593-611.

Moller, E. (1966) The chewing Apparatus. Acta Physio. Scand. 69, Suppl. 280.

Moss, M.L. and Young, R.W. (1960) A functional approach to craniology. Am. J. Phys. Anthropol. 18: 281-292.

Moss, M.L. (1971) Functional cranial analysis and the functional matrix. ASHA Reports 6: 5-18.

Moss, M.L. and Meehan, M. (1970) Functional cranial analysis of the coronoid process in the rat. Acta Anat. 77: 11-24.

Nanda,S.K., Merow, W.W. and Sassouni, V. (1967) Repositioning of the masseter muscle and its effect on skeletal form and structure. Angle Orthod. 37: 304.

Nikitiuk, B.A. (1964) A study of the temporal and masseter muscles: Influence on the skull form of the rhesus monkey (English translation). Trans. Moscow Soc. Nat. 14: 54-64.

Nikitiuk, B.A. (1965) Demonstration at VIII International Congress of Anatomists, Wiesbaden (August 1965).

Oyen, O.J. (1982) Masticatory function and histogenesis of the middle and upper face in chimpanzees (P. troglodytes). In Factors and Mechanisms Influencing Bone Growth, A.R. Dixon and B.G. Sarnat (eds.), Progress in Clinical and Biological Research, Vol. 101, pp. 559-568.

Oyen, O.J. (In preparation for Mondo Ortodontico) Postnatal growth of the facial skeleton: Part I, A consideration of what we (think) we know about how the face grows (translated by F. Magni).

Oyen, O.J., Walker, A.C. and Rice, R.W. (1979) Craniofacial growth in olive baboons (Papio cynocephalus anubis): Browridge formation. Growth 43: 174-187.

Oyen, O.J. and Enlow, D.H. (1982) Structural-functional relationships between masticatory biomechanics, skeletal biology and craniofacial development in primates. In Primate Evolution Biology, Proceedings of the VII Int. Cong. Primat., Springer-Verlag (Heidelberg). B. Chiarelli and R. Corruccini (eds.), pp. 93-97.

Oyen, O.J. and Russell, M.D. (1982) Histogenesis of the craniofacial skeleton and models of facial growth. In The effect of Surgical Intervention on Craniofacial Growth, J.A. McNamara, Jr., D.S. Carlson and K.A. Ribbens, (eds.). Craniofacial Growth Series, Number 12, Center for Human Growth and Development, University of Michigan, Ann Arbor, pp. 361-372.

Oyen, O.J. and Teaford, M.F. (In progress) Dental eruption and the concept of functional occlusion: An interpretation based on an in vivo study.

Partain, C.L., James, A.E., Rollo, F.D.,and Price, R.R. (1983) Nuclear Magnetic Resonance (NMR) Imaging. Philadelphia: W.B. Saunders.

Pavlicek, W., Modic, M., and Weinstein, M. (1984) Pulse sequence and significance. Radiographic 4: 49-65.

Petrovic, A. (1972) Mechanisms and regulation of mandibular condylar growth. Acta Morphol. Neerl. Scand. 10: 25-34.

Pratt, L.W. (1943) Experimental masseterectomy in the laboratory rat. J. Mammalogy 24: 204-211.

Purcell, E.M., Torrey, H.C., and Pound, R.V. (1946) Physics Review 69: 37.

Ralston, H.J. (1961) Uses and limitations of electromyography in the quantitative study of skeletal muscle function. Am. J. Orthod. 47: 521.

Rangel, R.D. (1984) Changes in Masticatory Biomechanics that Affect Growth and Development of the Facial Skeleton in the Vervet Monkey: Quantitative and Qualitative Analysis of Supraorbital Bone Remodeling. Master's Thesis, Department of Oral Biology, School of Dentistry, Case Western Reserve University, Cleveland, Ohio.

Rangel, R.D., Oyen, O.J. and Russell, M.D. (1985) Changes in masticatory biomechanics and stress magnitude that affect growth and development of the facial skeleton. In Normal and Abnormal Bone Growth Basic and Clinical Research, Dixon, A.R. and Sarnet, B.G. (eds.). New York: Alan R. Liss, Inc.

Ringquist, M. (1973) Isometric bite force and its relation to dimensions of the facial skeleton. Acta Odontogica Scandinavic 31: 35-42.

Russell, M.D. (1983) Browridge development as a function of bending stress in the supraorbital region. Am. J. Phys. Anthropol. 60: 248.

Schumacher, G. H. (1961) Funktionelle Morphologie der Kaumuskulatur. Gustav Fischer Verlag, Jena.

Sicher, H. (1965) Oral anatomy, Mosby, N. St. Louis.

Simpson, C.D. (1966) Experimental mandibular dysplasia. Angle Orthod. 36: 224.

Soni, N.N. and Malloy, R.B. (1974) Effect of removal of the temporal muscle on the coronoid process in guinea pigs: Quantitative triple fluorochrome study. J. Dent. Res. 53: 474-480.

Swenson, M.G. (1964) Complete Dentures, 5th ed. St. Louis: C.V. Mosby Co., p. 60.

Takada, K., Lowe, A.A., Freund, V.K. (1984) Canonical correlations between masticatory muscle orientation and dentoskeletal morphology in children. Am. J. Orthod. 86: 331-341.

Throckmorton, G.S., Finn, R.A. and Bell, W.H. (1980) Biomechanics of difference in lower facial height. Am. J. Orthod. 77: 410-420.

Walker, A.C. (1978) "Functional Anatomy of Oral Tissues." In Textbook of Oral Biology, J.H. Shaw, F.A. Sweeney, C.C. Capuccino, and S.M. Meller (eds.). Philadelphia: Saunders, 1978.

Ward, S.C., Beecher, R.M. and Corruccini, R.S. (1981) Effects of dietary consistency on craniofacial growth. Anatom. Recor. 199(3): 267A. Abstract.

Warwick, R. and Williams, P.L. (1973) Gray's Anatomy, 35th British Ed. Philadelphia: Saunders.

Washburn, S.L. (1947) The relation of the temporal muscle to the form of the skull. Anat. Rec. 99: 239-48.

Watt, D.G. and Williams, C.H.M. (1951) The effects of physical consistency of food on the growth and development of the mandible and the maxilla of the rat. Am. J. Orthod. 37: 895.

Weijs, W.A. and deJongh, H.J. (1977) Strain in mandibular alveolar bone during mastication in the rabbit. Archs. Oral Biol. 22: 667-775.

Weijs W.A. and Hillen B. (1984) Relationships between masticatory muscle cross-section and skull shape. J. Dent. Res. 63: 1154-1157.

Weijs W.A. and Hillen B. (1984) Relationship between the physiological cross-section of human jaw muscles and their cross sectional area in computer tomograms. Acta Anat. 118: 129-138.

Weijs W.A. and Hillen, B. (1985) Physiological Cross-section of the Human jaw muscles. Acta Anat. 121: 31-35.

Weijs W.A. and Hillen, B. (1986) Correlations between the cross-sectional area of the jaw muscles and craniofacial size and shape. Am. J. Phy. Anthropol. 70: 423-431.

Woodside, D.G., Metaxas, A. and Altuna, G. (1987) The influence of functional appliance therapy on glenoid fossa remodeling. Am. J. Orthod. and Dentofac. Orthop. 92(3): 181-198.

APPENDIX

Basic magnetic resonance imaging principles.

Magnetic resonance imaging technique is based on the presence of specific magnetic properties found within certain atomic nuclei (Purcell, 1946) (Figure A-1. Unless otherwise designated, this and all figures which follow are adapted from "Basic NMR Principles" by Partain, et al., as published in Radiograpics , January 1984.) The proton of the hydrogen nucleus is the simplest case. Under normal conditions, the spinning nucleus behaves like a magnet and generates a magnetic moment which is oriented in a random fashion (Figure A-2). In the presence of an external magnetic field, the magnetic moment will orient either parallel or in an antiparallel fashion to the poles of the applied magnetic field (Figure A-3). Placing the spinning proton in the magnetic field will cause the magnetic moment to precess or wobble. The frequency of this precession is called the Larmor frequency or resonant frequency (Figure A-4).

To perturb the static magnetic field, a radiofrequency signal at the resonant frequency is applied perpendicular to the main magnetic field (Figure A-5). When the magnetic field is thus altered by the radiofrequency signal, a change in the angle of precession of the spinning nucleus is induced. When the radiofrequency source is turned off, the net magnetization will realign itself with the main magnetic field. This change in the magnetic field produces currents (Figure A-6) which are detected by a receiver coil. The

91
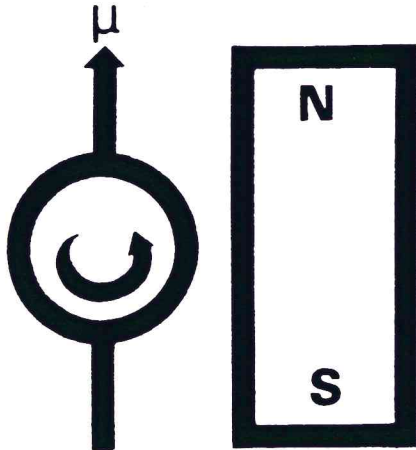
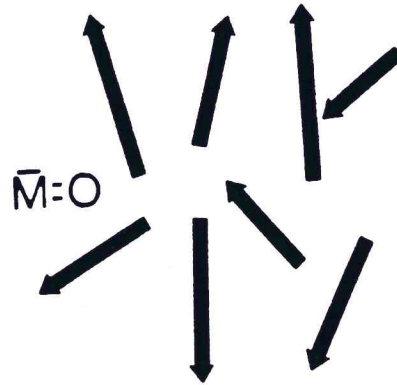Figure A-1. Magnetic properties found within atomic nuclei.

Figure A-2. Magnetic moment of spinning proton oriented in a random fashion.
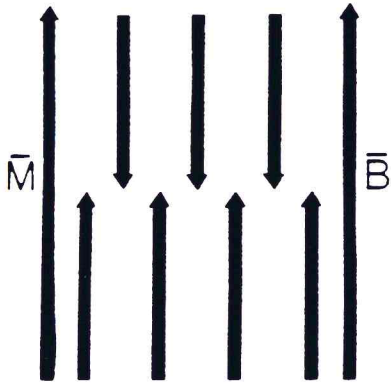

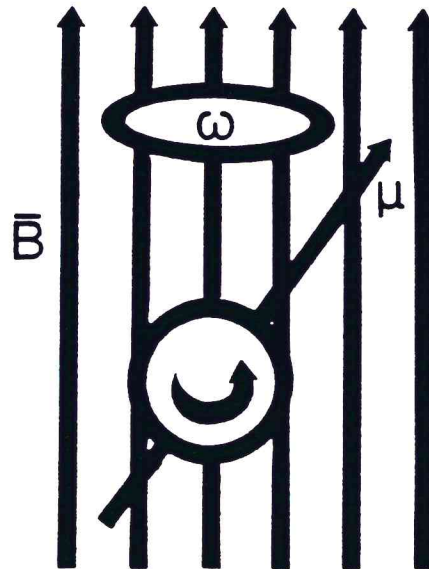Figure A-3. Magnetic moment oriented in parallel or antiparallel fashion.

Figure A-4. When placed in magnetic field, the nuclei will precess in the direction of magnetic field and rotate in their own axes.
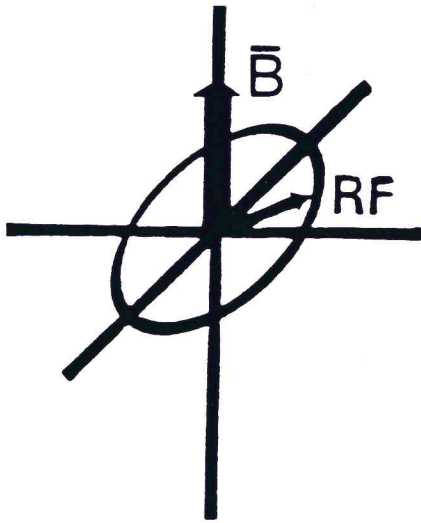
Figure A-5. Radiofrequency will be
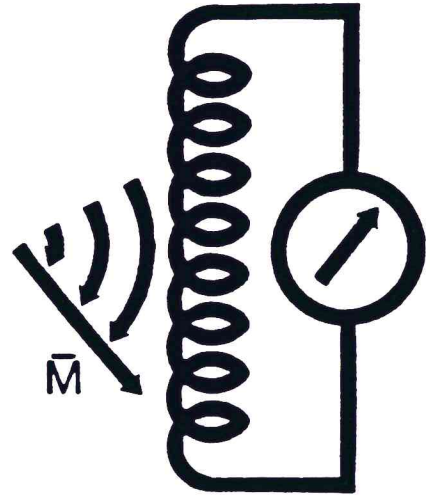applied perpendicular
perpendicular to the
magnetic field.

Figure A-6. By changing magnetic
field, currents will
be induced in the
receiver coil.
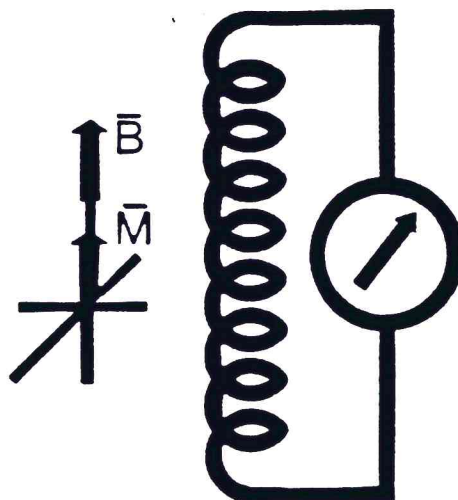
Figure A-7 When radiofrequency pulse
is removed, the net
magnetization will align
itself and return to
equilibrium.

radiofrequency coil is used for transmitting the radiofrequency pulse or receiving the magnetic resonance signals. The reduced currents produce the magnetic resonance imaging signal. As the net magnetization is restored to equilibrium (Figure A-7), the protons dispose of their acquired energy by two different processes designated T1 and T2. The rate of change of the signal as the protons return to equilibrium is exponential and is known as the spin-lattice relaxation. The time required for realignment is called T1 relaxation (spin-lattice relaxation time). The time for individual nuclei to lose phase coherence as they precess in an XY plane is called T2 (spin-spin relaxation time) (Figure A-8).

The magnetic resonance signal can be made to depend on either T1 or the T2 values of the protons. These values are different for different tissue types. The same anatomic structure can have different brightness in T1 weighted and T2 weighted images. T1 is very useful for studying normal anatomy because of the reconstruction it provides; T2 is useful in order to detect the pathology, but it does so at the expense of detail or resolution.

The maximum signal which can be induced occurs when the magnetic moment has been rotated into the XY plane at 90 degrees. This is known as a 90 degree excitation pulse.

Most magnetic resonance imaging systems utilize a spin echo technique to produce a maximum signal. The echo technique utilizes a 90 degree pulse followed by 180 degree pulse which refocuses the magnetization and produces a coherent "echo". The use of the echo
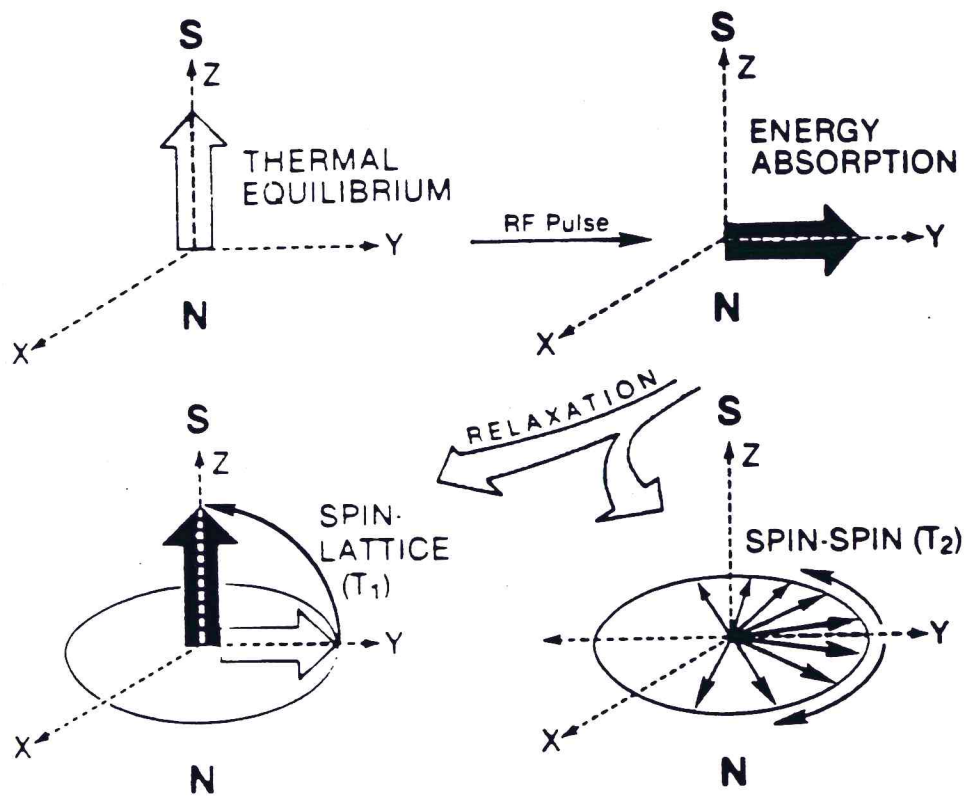
Figure A-8 T1 and T2
A radiofrequency pulse produces a net magnetization in XY plane. The loss of this magnetization involves two distinct relaxation processes: spin-lattice and spin-spin relaxation.

Spin-lattice relaxation is the return of magnetization to equilibrium with the applied magnetic field (Z direction) The time of this decay is characterized by the time constant T1.

Spin-spin relaxation is the loss of nuclear spin phase coherence. With a loss of phase coherence, the net magnetization in the XY plane converges to zero. The time for this process to occur is characterized by the time constant T2.

technique eliminates the effects of local static field inhomogenies
that cause the major dephasing and loss of signal following the 90
degree pulse.

In spin echo (SE) technique (Figure A-9), a pulse sequence is
initiated by applying a 90 degree pulse followed by a 180 degree
pulse. The time between the 180 degree pulse and the echo peak will
always equal the time delay between the 90 degree and 180 degree
pulses because rephasing requires as much time as dephasing.
Echotime (TE) is the time between the beginning of the 90 degree
pulse and the peak of the echo. The period of time between the
beginning of a pulse sequence and the beginning of the next pulse
sequence is defined as the repetition time (TR).

A field echo (FE) pulse sequence (Figure A-10) is one in
which the signal is rephased by the reversal applied magnetic field
gradients (a magnetic field which carries in strength in a certain
given direction. Gradient fields are used to encode the location of
the signals received from the object being imaged). The most useful
feature of field echo sequences is its extremely short repetition
time (TR) compared to spin echo sequences. Because of its simplicity
and its relatively short time requirements, the field echo pulse
sequence was used in this study.

The essence of tomographic imaging is that the signals arise
from a single plane or slice of the subject. It is possible to
confine the proton resonance effect to a thin slice of the subject by
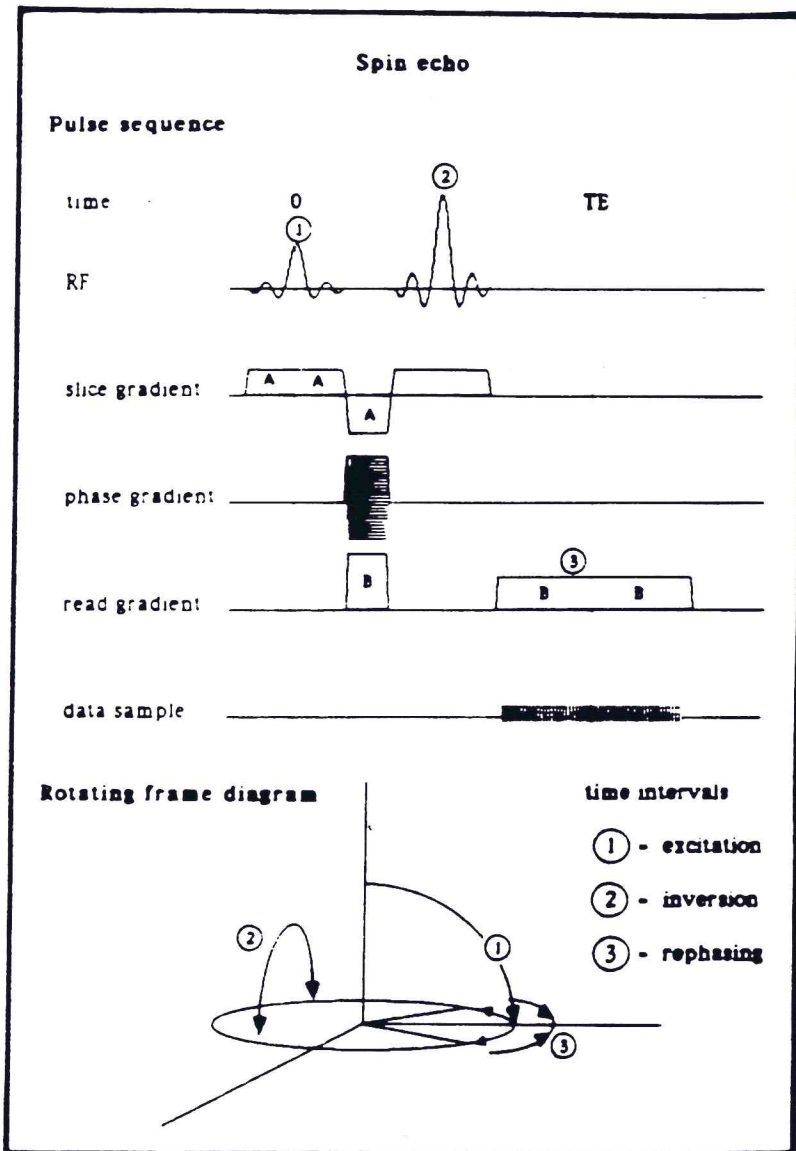applying a magnetic field gradient at the same time the
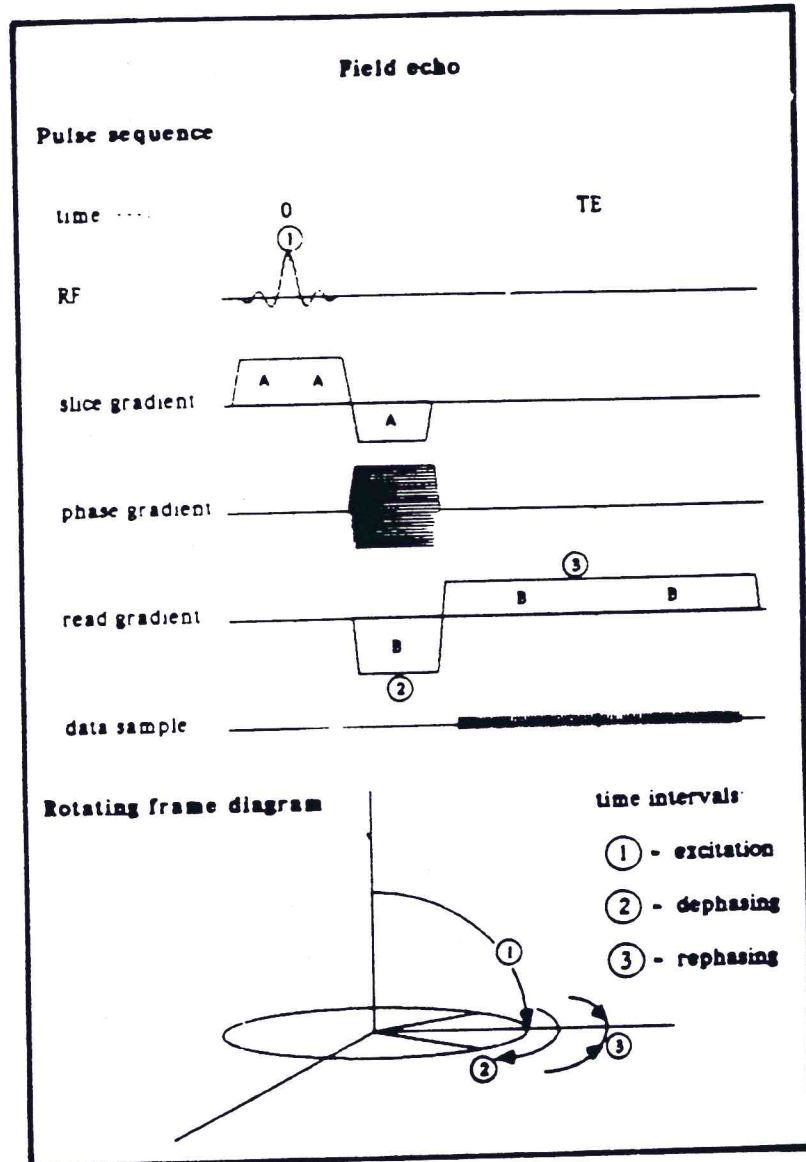
Figure A-9 Spin echo (SE) technique.

Figure A-10.   Field echo (FE) technique.

radiofrequency pulse is applied. The gradient ensures that the field strength is only correct for the resonant frequency of the pulse at plane of the slice. On either side of the selected plane, the field strength will be too high or too low for proton resonance. It also follows that the plane of the slice may be moved along the patient by altering the frequency of the radiofrequency pulse. Furthermore, the slice does not have to be a transverse cross section. By applying the gradient in another direction, it is possible to obtain proton resonance in coronal and sagittal planes. After resonance has been established in the slice, this gradient is switched off.

In order to construct an image of a cross-sectional slice of patient, it is necessary to determine from which part of the slice the signals are coming. This is done by applying a magnetic gradient across the slice while the signal is being received. The gradient ensures that the signals from the high field side of the slice will have a higher frequency than the signals from the low field side. When the signals are being processed to form the image, this frequency difference can be related to spatial position. Gradient magnetic fields are thus used to encode spatial information in two dimensions and to select the anatomical position of the slice in the third dimension.

The hardware used for magnetic resonance imaging is mainly associated with the magnet which produces the main magnetic field. Most magnetic resonance scanners use some form of electromagnet. The field is produced by a solenoid or series of coils and is normally

horizontal (Figure A-11). [This figure and all figures to follow are adapted from Magnetic Resonance Imaging, Basic Principles for Operators (David Blakeley, ed.), a publication of the Picker Clinical Science Center, 1985]. The evenness or homogeneity of the field is often affected by iron in the locality, but matters can be set to right by shim coils within the magnet. The field gradients, which have already been discussed, are produced by coils, usually mounted on the patient tube. The radio frequency coils for pulse transmission and signal reception are mounted close to the patient.

The most common type of magnet is called superconducting because its main winding is a niobium alloy super-conductor which has zero electrical resistance when cooled in a tank of liquid helium. These superconducting (or cryogenic) magnets are very stable, but, to maintain their operating temperature, they require a continuous supply of liquid helium and liquid nitrogen over quite a wide range, typically from 0.1 to 1.5 Tesla (1 Tesla = 10,000 Gauss). There are some helium recycling devices about to be introduced which will reduce and ultimately obviate the need for liquid helium replenishment.

The design of the gradient coils is an important feature of a magnetic resonance imaging system (Figure A-12). The gradient coils are the current-carrying coils designed to produce a desired gradient magnetic field. Large currents are passed through these coils for short periods and they form an integral part of the image acquisition process which is controlled by pulse sequence.
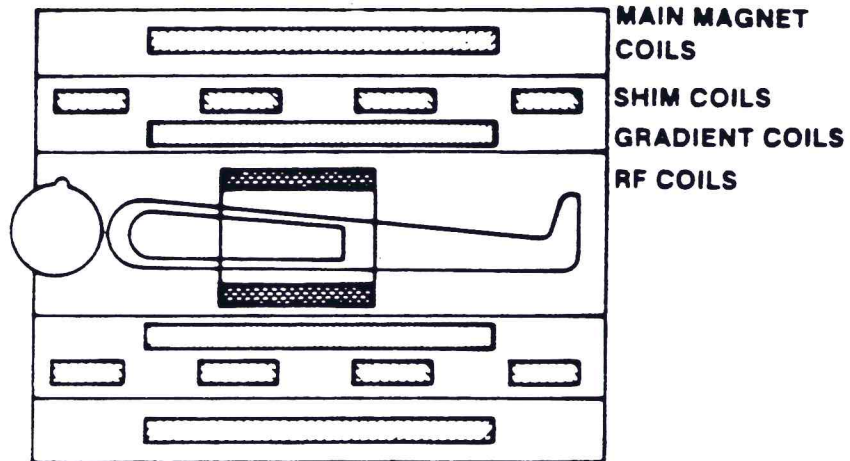
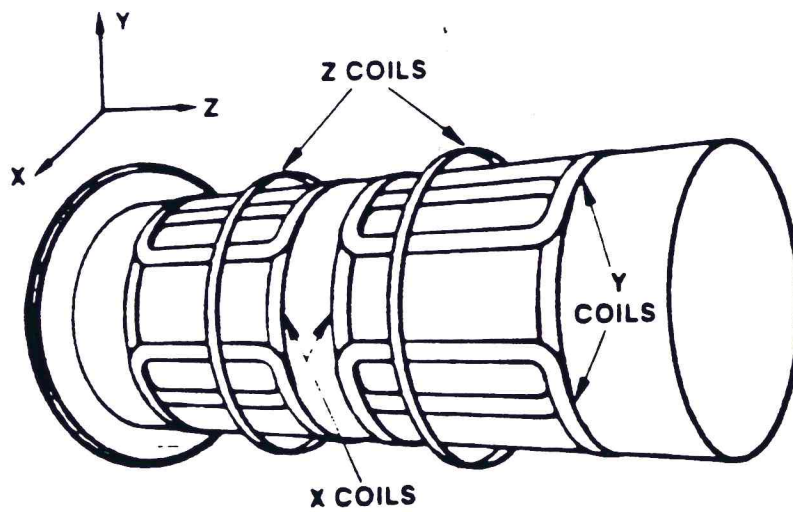Figure A-11. Series of coil used in magnetic resonance imaging.

Figure A-12. Gradient coils.

Radio frequency coils (Figure A-13) need to be as close to the patient as possible. When head scans are required, a smaller receiver coil is used. The use of small surface coils enables images to be produced that are a true representation of the limited field of view and receive a higher signal to noise ratio.

The operator and display console control all data acquisition, digital conversions and image processing. The control of the magnetic resonance imaging process is through a menu-driven software system. Image reconstruction takes about 5 seconds and uses a separate array processor to process the data.

The type of image obtained is decided by the sequence of radiofrequency pulses and gradient pulses which are applied during the acquisition period. The time for one acquisition may range from 2 to 20 minutes. Up to 16 contiguous images may be obtained in 5 to 6 minutes, depending upon the pulse sequence chosen. Slice thickness (Figure A-14) may vary from 2-20 mm. The desired thickness is selected by applying a magnetic field gradient across the intended slice, with the mid-frequency of the radiofrequency pulse adjusted to the larmor frequency of the center of the slice plane. The thickness of the slice is then dependent on the field gradient and the bandwidth of the radiofrequency pulse. In order to reduce slice thickness, it is necessary to increase the strength of the gradient or decrease the radiofrequency bandwidth. In spite of the apparent slowness of the imaging process, patient examination times are comparable to those for computed tomography. In addition, magnetic
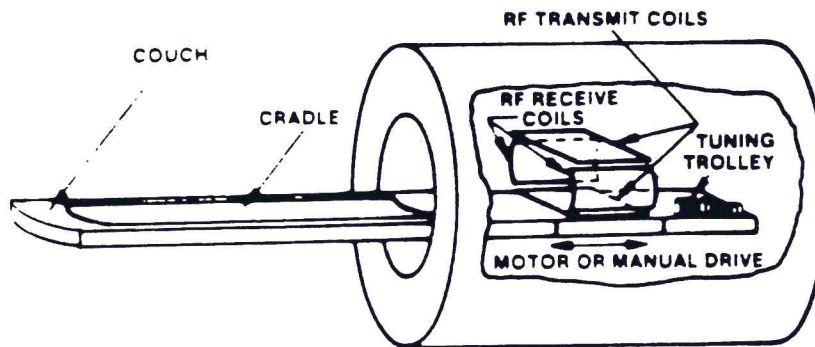
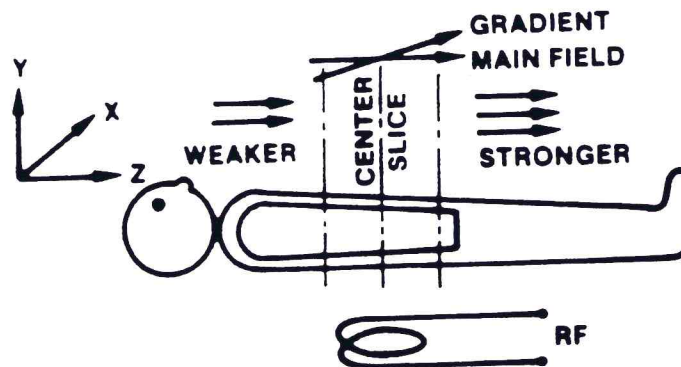Figure A-13.   Radiofrequency coil.

Figure A-14.   Slice selection and slice thickness.

resonance imaging offers greater inherent contrast, multiple simultaneous slices, and direct coronal and sagittal views.